

Regenerator Placement and Fault Management in Multi-wavelength Optical Networks

SHEN, Dong

A Thesis Submitted in Partial Fulfillment
of the Requirements for the Degree of
Master of Philosophy
in
Information Engineering

The Chinese University of Hong Kong

July 2011



Abstract

This thesis has addressed two important network design aspects of optical wavelength routing networks, namely, regenerator placement problem for translucent optical networks and fault monitoring in all-optical networks.

Regenerator Placement and Resource Allocation Optimization for Translucent Optical Networks

In this part, we have proposed a cost-effective design to reduce the required network deployment cost in translucent optical networks by adopting two modulation formats so as to achieve two different optical reaches (the maximum distance an optical signal can travel without O-E-O regeneration). Two cases representing two common scenarios, namely, ensuring any-to-any connectivity over the network and serving a forecast traffic demand matrix, have been investigated using multiple modulation formats. For the any-to-any connectivity case, we have tackled the regenerator placement problem with a two-step planning algorithm. In the second scenario, by proposing detailed and exact regenerator site architecture, accommodating a pool of back-to-back transponders, we have formulated an Integer Linear Programming (ILP) to minimize the overall network deployment CAPEX including the transponder cost and the regenerator site cost, coupled with routing and wavelength assignment task.

In the second part, we have investigated two practical problems. First, we have combined the important traffic grooming task with O-E-O regenerator placement, by

constructing an auxiliary graph, over which different grooming policies can be applied. Second, by constructing complex decision graph and running shortest path algorithm, our proposed solution could find the optimal wavelength assignment scheme compared to those intuitive schemes in terms of cost evaluated by the total number of O-E-O regenerators required for both signal regeneration and wavelength conversion.

Adaptive Fault Monitoring in All-Optical Networks Utilizing Real-Time Data Traffic

All-optical DWDM networks are vulnerable to physical failures, such as fiber cut, optical cross-connect (OXC) malfunction and optical amplifier breakdown. Due to the extremely large transmission capacity of all-optical networks, these possible failures may be translated to disastrous communication disruption. Hence, fault detection is one of the crucial aspects in network management to assure network reliability and availability. With the increased complexity of the network topology, fault detection and localization may incur significant management and operating costs. Thus, an efficient and cost-effective fault detection and localization system is highly desirable to assure the specified levels of quality of service. In this thesis, we have proposed a novel fault detection and localization scheme for all-optical networks with the information of the real-time data traffic. Our adaptive fault localization framework is based on combining passive and proactive monitoring solutions, together with adaptive management in two phases. Numerical results have indicated that our proposed scheme has good scalability, in terms of the number of

fault monitors required. Also, we have showed that our framework allows more flexible network design, and requires much less monitoring bandwidth when compared with the passive monitoring solutions.

摘要

本文主要解决两个重要的骨干光网络设计规划问题：半透明光网络中的光信号再生节点的选择和资源分配策略的优化设计，以及提出了一种全新的利用实时动态光路由信息，自适应的发送光路探针来完成组成光骨干网络的光纤的存活性的监控机制。

半透明光网络中的再生节点的选择和资源分配策略的优化设计：

本部分主要分成两个子问题。第一，在之前的半透明网络设计中通常假设只利用某一种光调制技术，而本文探讨了在两种常用的设计场景下利用两种光调制码型技术在半透明光网络规划中可能带来的成本节省优势。一种场景是为保证任何节点都能顺利和其他光节点通信，如何选择光信号的再生节点并决定相应节点的光接发器类型（对于不同的调制码型）以保证所投资的资源成本最低。对此，我们主要提出了一种涉及图论中 *connected dominating set* 的规划算法来有效的找到最优的结果。另一种场景是在给定整改网络的流量矩阵的情况下，我们提出了利用整数线性规划（ILP）来实现总体网络规划所耗成本的最小的资源分配设计，其中包括了再生节点和光路由选择以及波长分配的。第二个子问题主要从实际运营商的角度来考虑。首先，针对流量疏导（*traffic grooming*）和光信号的再生资源需求问题，我们设计了一种用辅助图把两者统一到一起做综合决策。其次，我们通过把波长分配策略和再生器的位置选择问题整合到一张决策图上的方式，完成了可观的网络成本节省。

自适应的全光网络存活性监控机制设计：

未来全光网络的生存性（*survivability*）和可靠性（*reliability*）是非常重要的特性，因为一旦有错误发生，如光纤的断裂或者光节点的损坏，都可能引起巨大的损失。因此，面对越来越复杂的网络服务要求和拓扑，一种高可扩展性和高性价比的全光网络错误监控机制十分必要。

本文提出并设计了一种全新的自适应的光网络存活性监控机制。我们的自适应光网络监控机制通过把被动式的监控光网络错误的设计原理和主动式的定位光网络错误的设计算法相结合的方式，充分利用实时的光路由信息和闲置状态的波长资源来实习自动控制全光网络的监控。大量随机网络拓扑的仿真结果显示我们提出的监控机制具有很好的可扩展性；通过在几个实际的网络拓扑上和被动式监控设计原理的仿真比较结果，我们的方法使用更加少的监控器并且非常容易适应拓扑结构的变化和演进。

Acknowledgements

First of all, I would like to thank my advisor Prof. Chan Chun-Kit for his constant guidance, support and encouragement. This thesis would not be possible without his knowledge, hard work, dedication to excellence and careful attention to details. The insightful discussions and invaluable reviews were of great benefits to my research experience. It has been an enlightening experience for me to do my research work under his extraordinary supervision.

I would like to thank Prof. Chen Lian-Kuan for his valuable comments, discussions and support on my research and studies.

Also, I would like to thank Dr. Li Guangzhi, Dr. Wang Dongmei, Dr. Xu Daihai and Dr. Robert Doverspike for giving me the opportunity to conduct research in AT&T-Labs Research under their patient help and insightful guidance.

I am very fortunate to work with a group of excellent students and research staff in the Lightwave Communications Lab of CUHK, including Qiu Yang, Xu Jing, Zhang Shuqiang, Jordan Tse, Dicky Tse, Jia Wei, Li Pulan, Liu Zhixin, Francis Yuen, Wang Qike, Luk Hon-Tong and Dr. Li Ming.

I owe a lot more than a thank to my family. Without their love and encouragement, I would not be able to move one single step in my life.

Table of Contents

Abstract	i
摘要.....	iv
Acknowledgements	v
Table of Contents	vi
Chapter 1 Background.....	1
1.1 Translucent Optical Networks	1
1.1.1 The Way Towards Translucent	1
1.1.2 Translucent Optical Network Architecture Design and Planning.....	3
1.1.3 Other Research Topics in Translucent Optical Networks.....	6
1.2 Fault Monitoring in All-Optical Networks	12
1.2.1 Fault Monitoring in Network Layer’s Perspective.....	12
1.2.2 Passive Optical Monitoring.....	14
1.2.3 Proactive Optical Monitoring.....	16
1.3 Contributions.....	17
1.3.1 Translucent Optical Network Planning with Heterogeneous Modulation Formats	17
1.3.2 Multiplexing Optimization in Translucent Optical Networks.....	19
1.3.3 An Efficient Regenerator Placement and Wavelength Assignment Scheme in Translucent Optical Networks	20
1.3.4 Adaptive Fault Monitoring in All-Optical Networks Utilizing Real-Time Data Traffic	20
1.4 Organization of Thesis	22
Chapter 2 Regenerator Placement and Resource Allocation Optimization in Translucent Optical Networks.....	23
2.1 Introduction.....	23
2.2 Translucent Optical Network Planning with Heterogeneous Modulation	

Formats.....	25
2.2.1 Motivation and Problem Statements	25
2.2.2 A Two-Step Planning Algorithm Using Two Modulation Formats to Realize Any-to-Any Topology Connectivity.....	28
2.2.3 Illustrative Examples.....	30
2.2.3 ILP Formulation of Minimizing Translucent Optical Network Cost with Two Modulation Formats under Static Traffic Demands.....	34
2.2.4 Illustrative Numeric Examples.....	42
2.3 Resource Allocation Optimization in Translucent Optical Networks	45
2.3.1 Multiplexing Optimization with Auxiliary Graph.....	45
2.3.2 Simulation Study of Proposed Algorithm	51
2.3.3 An Efficient Regenerator Placement and Wavelength Assignment Solution	55
2.3.4 Simulation Study of Proposed Algorithm	60
2.4 Summary	64
Chapter 3 Adaptive Fault Monitoring in All-Optical Networks Utilizing Real-Time Data Traffic	65
3.1 Introduction	65
3.2 Adaptive Fault Monitoring.....	68
3.2.1 System Framework	68
3.2.2 Phase 1: Passive Monitoring	70
3.2.3 Phase 2: Proactive Probing	71
3.2.4 Control Plane Design and Analysis.....	80
3.2.5 Physical Layer Implementation and Suggestions	83
3.3 Placement of Label Monitors	83
3.3.1 ILP Formulation	84
3.3.2 Simulation Studies	86
3.3.3 Discussion of Topology Evolution Adaptiveness.....	93
3.4 Summary	95
Chapter 4 Conclusions and Future Work	96

4.1 Conclusions	96
4.2 Future Work.....	97
Bibliography.....	98
Publications during M.Phil Study	105

Chapter 1 Background

Nowadays, as the information technology evolves, the underlying global backbone network infrastructure is facing increasing challenges. The continuous and rapid growth in traffic demand of Internet backbone have been driven by the trend to maximize information technology benefit, such as the mobile broadband industry which is estimated to have 50 billion connections by 2020, the exploding online HD video streaming services, as well as the revolutionary cloud enabling service. Optical networks adopting Wavelength Division Multiplexing (WDM) technology are considered to be the best choice for the backbone network of Internet. With WDM, a single fiber is capable of carrying up to hundreds of parallel optical wavelengths each of which carries up to 100 Gbps. In this chapter, we will introduce some important problems in optical WDM networks.

1.1 Translucent Optical Networks

1.1.1 The Way Towards Translucent

In the current academic literature of optical networking, a network is referred as transparent if all the nodes on the network are equipped with all-optical cross connects (OXC) or reconfigurable optical add-drop multiplexer(ROADM) without any electronic regeneration function. Each light-path must be routed from its source to its destination without any electronic processing at intermediate nodes en route. A transparent optical network possesses the advantage of modulation format

transparency, bit-rate transparency and protocol transparency. Despite these great advantages, a transparent network at current stage, however, suffers from the physical layer impairments induced by the underlying transmission fiber system, such as chromatic dispersion, polarization mode dispersion, nonlinear effects, and crosstalks, especially when the transmission data rate increases from 10Gbps to 40Gbps and 100Gbps. These largely limit the route distance and flexibility of the network. The opposite of a transparent network is a so-called opaque network in which all channels are detected at each node, and their corresponding payloads are then electronically regenerated and switched to any new outgoing wavelength. Although there is no reach constraint for an opaque network, the tremendous cost to deploy fully-capable electronic switching at each node prohibits large scale network rollout.

To seek a graceful balance between network design cost and service provisioning performance, translucent optical network architecture has been proposed [1]. Generally, it uses a set of sparsely but strategically placed electronic regeneration resource, which is used to provide 3R function, namely, re-amplify, re-shape, and re-time, to the optical signals so that the optical signals can travel for another long path until reaching the next node with regeneration resource or the corresponding destination. Rather than using purely optical or electronic switching, a translucent optical network is a compromise between all-optical switching and all-electrical switching, showing the inherent cost-effective property together with the ability to overcome the physical impairment limitations.

1.1.2 Translucent Optical Network Architecture Design and Planning

Clearly, the first consideration in translucent network design is about how to plan the regeneration resource, in the WDM networks, subject to specific service provision requirements. Currently, three major types of architecture, island of transparency, sparsely placed regeneration sites, and selective regeneration, have been proposed in the literature, and will be introduced in the following sub-sections.

Island of Transparency

In the architecture known as 'island of transparency' [2], a large-scale optical network is divided into several domains (i.e. islands) of optical transparency. In the same domain, a light-path can transparently reach any node without any intermediate signal regeneration. However, for communications between different domains, electronic switches (ESs) are used at the domain boundaries. These switches act as 3R regenerators and wavelength converters in addition to relaying the light-paths crossing the domain boundaries.

Partitioning a large transport network into several small sub-networks can simplify network control and management, as each sub-network can be maintained individually. Moreover, it matches the concept of operator domain that the operator could deploy equipments from different vendors, regardless of the interoperability capability. Also, even for a single vendor system, the isolation allows carriers to upgrade network capacity separately on independent time scale.

The key disadvantage of this island of transparency scheme is its extra regeneration induced by the simple and flexible nature of the architecture, indicating a trade-off between operational cost and capital cost.

In such type of translucent network, one important issue is how to efficiently and economically partition a large-scale optical network into several sub-networks. The input of the problem would be the original physical topology and optical reach, and the objective is to minimize the number of island border nodes. Based on the original work of A. Saleh [2], Karasan & Arisoylu [3] addressed the transparent domain partition by employing an ILP model and a heuristic to continuously merge the graph faces to clusters (i.e. transparent islands) to minimize the number of total divided transparent islands. In [4], Shen, Wayne and Tucker further studied a more detailed design taking the ASE noise into optical reach evaluation model and proposed an efficient island-division approach.

Sparsely Placed Regeneration Sites

A translucent optical network can be more general than island of transparency architecture, in which a set of nodes are selected to have regeneration capability, named as regeneration site. If a connection route is too long to be carried in only optical domain, then it must go through one or more regeneration sites. Within the regeneration site, two potential implementation methods have been studied. Either all the traffic transiting these sites needs to do O-E-O conversion, or they have optically by-pass function so that regeneration only occurs when needed.

Rather than partitioning the network into sub-networks as in the island of transparency architecture, the chief objective of this design principle is to strategically choose the designated regeneration sites from all the network nodes. A range of heuristic solutions have been proposed to solve the problem. Yang and Ramamurthy [5] proposed heuristics such as “nodal degree first,” “centered node first,” etc, to allocate regeneration sites, specifically for the network cases with topological information only and more information on forecast traffic information. Another strategy aimed to place the minimum number of regeneration sites while ensuring any-to-any connectivity, subject to certain optical reach over the network, was first presented in [6], and later was proved to be NP-Complete in [7]. It modeled the regeneration sites allocation problem to be equivalent to compute the minimal Connected Dominating Set (CDS) of an auxiliary topology. Due to the fact that NP-Complete Problem is computational intractable, some heuristics [6] are proposed to handle large scale network cases.

Selective Regeneration

The third investigated design option is so-called selective regeneration, allowing all the nodes to perform regeneration and regenerating a demand when needed. The regeneration decision is made per demand, together with the flexibility of choosing regeneration locations, thus yielding the fewest regeneration times needed. This strategy is commonly advocated and employed by the current telecommunication industry carriers [8]. Not much previous work was dedicated to this area of translucent network design, although we believe there are still many interesting

problems and optimization margin remaining to be explored in academic research.

1.1.3 Other Research Topics in Translucent Optical Networks

Light-path Routing and Wavelength Assignment

With the chosen translucent network architecture, the next task that a carrier faces, is to maximize its investment by attracting more clients and satisfying their demands, which is usually denoted as routing and wavelength assignment (RWA).

For the island of transparency architecture, the issue becomes how to establish light-path connections that may exist within a single island or traverse multiple transparent islands. It is straightforward to route light-path services between a pair of nodes within the same transparent island, using the shortest path routing algorithm or other routing and wavelength assignment algorithms developed in transparent networks. Furthermore, for a node pair requests across several islands, a hierarchical routing strategy has been proposed to efficiently choose routes across multiple domains [1]. Such hierarchical strategy models the translucent network in two layers, with top one including all abstract island nodes and the bottom one containing extended information of each abstract node. Based on such a model, light-path routing and wavelength assignment was implemented in two steps from the top layer to the bottom layer. Ideally, a route that transited the minimum number of transparent islands was first found in the top layer, and a transparent path between the two border nodes was searched at the transit abstract border node.

Most of the research effort in light-path routing and wavelength assignment within

translucent optical networks has been devoted to sparsely placed regeneration sites case, which can be further divided into two categories by the assumed traffic nature. For the static case, a set of light-path demands or a forecast traffic matrix, the system optical reach as well as the topology are given, the objective is to serve the maximal number of demands or minimizing the consumed resource after satisfying all the demands. Tang in [9] presented a complete ILP formulation to address the regeneration site selection and RWA simultaneously by introducing a graph transformation scheme. Mayssa in [10] proposed a heuristic called Cross Optimization for RWA and Regenerator Placement (COR2P), tackling the problems separately and step-by-step. As for another well-investigated case, under the stochastic nature of dynamic traffic demands assumption, the aim was to minimize the request blocking probability. In [5], algorithms such as fragmentation, trace back, and hybrid weighted shortest path first were shown and evaluated with simulation results. Besides, a 2D-Dijkstra's algorithm that jointly considered both topological and wavelength information in [11] was used to route the dynamic traffic demands.

Survivability in Translucent Optical Networks

Same as all other networks, survivability issue also plays a crucial role in translucent optical network design and operations, as the clients' services and applications are all counting on the reliability of the infrastructure network. Specifically, due to the tremendous bandwidths that a single fiber link carries enabled by WDM technology, the penalty induced by any fiber link or node failure could be prohibitive, making the survivability even more important in optical backbone networks.

Various proposed approaches to support survivability in transparent WDM networks can be generally divided into protection and restoration techniques. Protection techniques use pre-assigned and extra bandwidth to assure survivability, which are also referred as proactive approaches. In contrast, restoration techniques reroute the affected traffic after a failure happens. Protection techniques can be further divided into link, segment and path protection. They can also be divided into dedicated and shared protection based on whether the backup network resource is allowed to be shared by different traffic or not. Restoration techniques can also be divided into link, segment and path restoration.

In order to employ protection technique, a straightforward way to provide survivability in translucent networks, is to put these pre-assigned protection light-paths into the original working light-paths planning stage, equivalent to have a set of extra demands to be served. The work in [12] addressed the issue of survivability in optical mesh networks considering optical layer protection and realistic optical signal quality constraints. Three kinds of resource sharing scenarios, including wavelength-link sharing, regenerator (i.e. OEO) sharing among protection light-paths, and regenerator sharing between working and protection paths, were investigated in this work. On the other hand, restoration design principle can also be applied. For instance, the authors in [13] notice it is technically easier to assume failure detection at the opaque nodes only and thus natural to consider viewing the transparent path segments between opaque nodes as the entities to be protected for network survivability, as opposed to single spans or entire end-to-end paths in

translucent optical networks, inspiring them to explore the segment-based scheme by formatting the restoration capacity planning problem as an ILP.

Traffic Grooming in Translucent Optical Networks

Regarding the discrepancy between the client request bandwidths, of which a large portion are at lower bit rate like OC-3, OC-12, or OC-48, and the underlying light-path channel capacity up to OC-192 or even higher, it is necessary to multiplex these diverse low-speed requests into light-paths with an efficient strategy, so as to maximize the utilization of the network. The problem, denoted as traffic grooming task in optical WDM networks, has been extensively studied.

Traffic grooming in translucent optical networks differs from the conventional situation where an ideal optical layer is assumed. In another word, we have to put the optical reach constraint into consideration when dealing with the same problem in translucent networks. Furthermore, previously, all the studies assumed all the nodes own the traffic grooming capability, depending on which a lot of works are done in either static traffic case or dynamic traffic case, with the objective to minimize the network resource consumed, maximize the served traffic demand number [14] or reduce the blocking probability [15]. Then, in [16], Zhu's investigation have indicated that an optical network with sparse traffic grooming capability would achieve performance close to that of a network with full range of traffic grooming capability on each node, where sparse traffic grooming capacity means only a few nodes had the traffic grooming capacity. Zhu's work [16] inspired Shen and Tucker

to look into the sparse traffic grooming problem in translucent optical networks, of which the opaque nodes set within the network were naturally selected to have traffic grooming capacity [17]. They examined how the number of opaque switch nodes and their placement affected the performance of traffic grooming. Their simulation studies indicated that with an increase in the number of opaque switch nodes, the performance of sub-wavelength traffic grooming was improved, as expected. Moreover, performance improvement saturated with an increasing number of opaque switch nodes under some networks topologies. However, this trend was not general for any type of topology. This study was claimed to be the first attempt dedicated to sparse traffic grooming in a translucent optical network. The study in [17] was based on the sparsely placed regeneration site architecture, as presented in the previous section, while the paper [8] from Shen investigated the traffic grooming problem in selective regeneration architecture taking the optical reach into constraint. They proposed an efficient heuristic by grabbing the neck of the light-path method. It was interesting to notice their attempt to distinguish layer-zero regeneration, represented by a 3R O-E-O regenerator with no traffic grooming capacity, between layer-one regeneration using a pair of back-to-back transponders allowing electronic packets processing.

In general, more attention should be paid to this area, as the scenario combining both traffic grooming and physical layer impairments is quite of practical concerns

Exploring the Wavelength Conversion Functions of Regeneration

It is well known that O-E-O conversion function provided by regeneration module could easily be coupled with wavelength conversion ability, without loss of generality. The wavelength-continuity constraint, refers that a given light-path connection should be composed of identical wavelengths on the links traversed by the light-path imposed on the RWA problem in optical networks. Thus, a potential investigation problem is how to explore this inherent wavelength conversion function to mitigate the wavelength-continuity constraint while planning regeneration modules into the translucent networks.

Regardless of the physical layer impairment, former studies, have already dedicated a lot of efforts on how to place wavelength converters sparsely to solve the wavelength contention problem induce by the wavelength-continuity constraint [18]. Nevertheless, some but not much original work have focused on the combination of regenerator placement and wavelength assignment. In [5], Yang's routing algorithm did consider the wavelength conversion capability of regenerators although his placement algorithm did not. In another study [19], regardless of its original aim, Angela L.Chiu did try to address the regenerator placement and wavelength assignment consideration together, by choosing the regenerator combination which minimized the sum of the inverse of available wavelengths over all separated light-paths. More research in this area is expected to strike a graceful balance between wavelength conversion and signal regeneration.

1.2 Fault Monitoring in All-Optical Networks

As stated in the abstract part, all-optical networks are vulnerable to physical failures, such as fiber cut, optical cross-connect (OXC) or ROADM malfunction and optical amplifier breakdown. Due to the extremely large transmission capacity of all-optical networks, these possible failures may be translated to disastrous communication disruption. Hence, fault management is one of the crucial aspects in network management to assure network reliability and availability. All the other network management modules, such as configuration management, security management, performance management and account management, are counting on the information provided by the fault detection and localization subsystem. In this section we will present some basic building blocks in fault management in all-optical networks, followed by current fault detection and localization research trends. In this thesis, we mainly focus on the fault detection and localization task in fault management.

1.2.1 Fault Monitoring in Network Layer's Perspective

Basically, fault monitoring can be provided either in those upper layers in the network, e.g., ATM, IP, SONET, SDH, etc, or in the optical layer individually. In addition, they can be provided together in a cross-layer manner [20]. The decision generally depends on the tradeoff between the required hardware cost and the fault detection time, and may differ from case to case in practical network implementations. The fault monitoring schemes in each layer, have their own functionalities and characteristics. As an example, in SONET networks, the

network-management system employs mechanisms such as BER measurement, optical trace, and alarm management to perform fault management at each node. In particular, these functionalities may be carried over various types of optical-layer overhead [21], including pilot tone, subcarrier-modulated overhead, optical supervisory channel, rate-preserving overhead, and digital-wrapper overhead. However, all these overheads are detected at some intermediate nodes along the light-path, which may not be acceptable in all-optical networks. In the case of higher layer, fault management mechanisms in some routing protocols such as IS-IS (Intermediate System-Intermediate System) and OSPF (Open Shortest Path First) use update messages to identify inter-domain and intra-domain routing failures[22].

Compared with optical layer monitoring schemes, upper layer protocols required less hardware support but more signaling efforts for fault monitoring. As a result, optical layer monitoring schemes generally respond much faster to a failure event, thus is preferred in achieving fast failure localization. Specifically, if we further restrict the dominant failure scenario to be the fiber-cut, which is common in optical WDM networks, optical layer fault monitoring becomes even more advantageous as such fiber-cut failure usually leads to much more fault alarms in upper layer monitoring schemes than in optical layer monitoring.

In the following introduction, we will throw our efforts to optical layer fault monitoring schemes review, in particular, to monitor fiber-link failures.

1.2.2 Passive Optical Monitoring

Currently, in all-optical WDM networks, employing optical layer monitoring scheme, a link failure is detected and localized simply based on the on-off status of some supervisory optical signals. This requires additional wavelength channels to transmit the supervisory optical signals, and some special devices called monitors [23] to check the on-off status and generate alarms upon a failure event. This incurred hardware cost is necessary for achieving fast link failure localization at the optical layer, and has to be minimized. Generally, the monitor generates the events - alarms, as inputs to the fault diagnosis engine, which could be a fault-to-link mapping database. Using various algorithms, the fault diagnosis engine identifies a set of network elements whose failures may have caused the input alarms. Due to the passive nature of waiting for alarms from monitors, this type of monitoring scheme is called as passive optical monitoring in this thesis, although there is no standard definition in the literature. There are two common passive optical monitoring schemes, namely, monitoring-cycle (m-cycle) and monitoring trail (m-trail).

Monitoring Cycle (m-cycle)

At first, when there is not so many links in the optical networks, a link-based monitoring scheme would be enough, where each individual optical link needs a dedicated monitor. Obviously, 100% link failure localization can be easily ensured in this case. However, as the optical WDM network scales from ring topology to mesh topology, the excess hardware cost and the network management cost associated

with the ever-growing number of monitors, in this link-based scheme, hinder its large scale adoption for future WDM networks.

In order to mitigate this problem, researchers have proposed to predefine a set of supervisory light-paths and assign one monitor to each of them. In such situation, one monitor is capable of generating alarm upon any link failure on the supervisory light-path. Those alarm signals can be denoted by a binary alarm code, in which each binary bit indicates whether the corresponding monitor alarms or not. If the set of supervisory or monitoring light-paths are properly allocated such that each link failure will trigger alarms in a unique set of monitors, then the failure can be localized by identifying the unique alarm code. With this design principle, the number of monitors placed would be largely reduced.

At this stage, the major design issue is how to design such supervisory light-paths in the WDM networks. The first attempt employing the above monitoring idea in [24], introduced the concept of simple m-cycle, where a set of simple cycles, each mapped to a specific light-path, were found to cover the network topology. A simple m-cycle was an optical loopback of supervisory wavelengths and it passes through each on-cycle node exactly once. Based on this work, ILP formulation and heuristic are presented in a series of works in [25]. The m-cycle concept was also extended to non-simple m-cycle in [26]. A non-simple m-cycle is allowed to pass through a node multiple times. In particular, non-simple m-cycles could better explore mesh connectivity of a network than simple m-cycles due to the more flexible monitoring structure, therefore bringing better cost saving margin.

Monitoring Trail (m-trail)

Both simple m-cycle and non-simple m-cycle used the cycle as the monitoring structure. Despite its simplicity and the beauty of cycle, the monitoring structure, essentially a light-path in WDM networks, is not necessarily a cycle. On the contrary, A line or a trail structure should match the nature of a monitoring light-path in a better way. Motivated by the observation, Wu and Ho made their exploration of monitoring trail design in [27]. It differed from simple and non-simple m-cycles by removing the cycle constraint, and thus an m-trail would be taken as an acyclic supervisory light-path with an associated monitor equipped at the destination node of the m-trail. A m-trail could also pass through a node multiple times. Clearly, m-trail provided the most flexible monitoring structure in utilizing mesh connectivity of the optical WDM network, and therefore required the minimum monitoring cost compared with other optical layer monitoring schemes.

1.2.3 Proactive Optical Monitoring

Another design principle, in contrast to passive optical monitoring, is denoted as proactive optical monitoring. Generally in proactive optical monitoring, optical probe signals are sequentially sent along a set of designed light-paths, and the network state is inferred from the result of this set of optical probe measurements [21]. The design objective is to minimize the diagnosis effort, the average number of probes, to locate failures.

To the best of our knowledge, Yonggang Wen and Vincent Chan[21] were the first

group of researchers studied the details of proactive probing scheme in all-optical network fault monitoring. In [21], by establishing a mathematical equivalence between the fault-diagnosis problem and the source-coding problem in information theory, an information theoretic approach were reported, where probabilistic link failures were localized by analyzing the syndromes of the minimum number of probe signals. A class of run-length probing schemes with low computation complexity was then developed to handle such network diagnose problems. However, limited by the inherent sequential nature of run-length probing scheme, the number of probing steps might be quite large for some network failure patterns and/or in some large networks, thus it might take a relative long time to localize the failure, which might not be acceptable in all-optical networks. Motivated by the shortcomings, they further proposed the non-adaptive fault diagnosis scheme in [28]. Instead of sending optical probing signals sequentially, a pre-determined set of probing signals were sent in parallel to probe the network state of health, through which the step of proactive probing would be largely reduced.

1.3 Contributions

1.3.1 Translucent Optical Network Planning with Heterogeneous Modulation Formats

As discussed above, the most significant difference between translucent and transparent optical networks is the maximum distance that the optical signal can travel without regeneration due to the physical layer impairment, denoted as optical

reach. To overcome this constraint, expensive O-E-O regeneration module is needed to be deployed in translucent optical networks. A major portion of research effort has been dedicated to finding the most cost-effective regeneration module placement method. However, most of the researchers in translucent optical network planning usually put too much attention in designing extremely complex planning algorithm as to reduce the cost in network layer.

In this thesis, under the sparsely placed regeneration sites architecture, we argue that by taking a cross-layer perspective, considerable network deployment cost saving can be achieved. Specifically, almost all the previous works assumed that only one type of optical modulation format was employed in the transmission system. Recently, many advanced modulation formats have been developed in optical transmission system and they have different optical reaches. Here, to the best of our knowledge, we have made the first attempt to explore the opportunity to use two modulation formats/two optical reaches in optical translucent optical network planning problem.

In the following chapter, we will address the translucent optical network planning problem in two different scenarios.

First, in order to realize any-to-any connectivity in a typical translucent optical network, where “connectivity” means that at least one physical layer impairment feasible path exists in the network, we have proposed a two-step planning algorithm to choose the regeneration nodes and nodes for different modulation format. Then

with the two-step algorithm, we have compared the overall cost of the case employing two modulation formats and the cases applying either one of the modulation formats individually. The result has shown that our design principle and algorithm can further reduce the planning cost.

Secondly, given the traffic matrix consisting of a set of light-path requests, the network topology and two optical reaches, we have formulated an ILP to minimize the network deployment cost involving optical transponders and regeneration site cost, coupled with routing and wavelength assignment. The novel point of our ILP is that we put both the capital and operational cost in translucent optical networks into the formulation. Several network cases have been considered to verify our formulation.

1.3.2 Multiplexing Optimization in Translucent Optical Networks

In this section, we have proposed a graph-based solution to the traffic grooming problem discussed in section 1.1.3. We use multiplexing optimization to denote the section, since the original problem is from the telecommunication industry, in which the term multiplexing is used for representing the traffic problem. As mentioned in section 1.1.2, the carriers usually prefer the selective regeneration architecture due to its flexibility, low cost and the well match to the business model. Thus, we have propose a novel multiplexing graph model and multiple multiplexing policies to perform low-bandwidth-connection routing and multiplexing optimization in DWDM mesh networks, combined with the incremental traffic model and physical

layer constraints. Based on this graph model, we can automatically determine where to route over the network, where to use existing available multiplexing wavelength connection channels, whether/where to create new multiplexing wavelength connections, where to add regenerators, and what is the overall investment cost: all the information a planner would like to know.

1.3.3 An Efficient Regenerator Placement and Wavelength Assignment Scheme in Translucent Optical Networks

We have shown that not much research effort has been dedicated to explore the wavelength conversion capability of regeneration module in section 1.2.3. In this part, we provide a novel auxiliary graph model to combine regenerator placement and wavelength assignment together. By assigning the right cost weight to the auxiliary graph edges, we can easily decide where to place regenerators and which wavelength to select by running the least cost algorithm over the graph, such that the overall number of regenerators required is minimized.

1.3.4 Adaptive Fault Monitoring in All-Optical Networks Utilizing Real-Time Data Traffic

Based on the introduction of passive and proactive optical monitoring schemes, we can identify their drawbacks as follows.

For passive optical monitoring, as the network topology is becoming more complex, much effort has to be made to design a feasible m-cycle coverage solution. Furthermore, even if a feasible cycle set is found, the cost of the required monitors is

quite substantial. Besides, the extra monitoring bandwidth cost is also getting high, as each monitoring cycle requires one distinct wavelength in an all-optical WDM network. For proactive probing scheme, it can only be applied to Eulerian networks, each of which contains an Euler trail (a path containing all the links without repetition). Although the authors in [21] have further improved their scheme to accommodate node failures and have demonstrated that all network topologies could be transformed to Eulerian networks, it is still unrealistic to configure the switching nodes to meet the requirements, as it may disrupt the existing connections and may largely increase the management cost. Besides, the requirement on the probing time and frequency is still not yet resolved.

Motivated by the pros and cons of both passive and proactive detection solutions, we propose a novel fault detection and localization scheme for all-optical networks with the information of real-time data traffic. Our adaptive fault localization framework is based on combining passive and proactive monitoring solutions, together with adaptive management in two phases. Numerical results from solving a simple monitor placement ILP have indicated that our proposed scheme has good scalability, in terms of the number of fault monitors required. Also, we have shown that our framework allows more flexible network design, and requires much less monitoring bandwidth when compared with the passive monitoring solutions.

1.4 Organization of Thesis

Chapter 2 discusses the translucent optical network planning by employing heterogeneous modulation formats under two commonly referred scenarios with sparsely placed regeneration sites architecture. Also, chapter 2 presents a graph-based solution for traffic grooming optimization problem, and an integrated regenerator placement and wavelength assignment scheme by building an auxiliary graph, both of which are under the selective regeneration architecture in translucent optical networks.

Chapter 3 presents an adaptive fault monitoring in all-optical networks utilizing real-time data traffic, by combining the passive and proactive monitoring ideas.

Chapter 4 concludes this thesis and suggests the possible future research topics.

Chapter 2 Regenerator Placement and Resource Allocation Optimization in Translucent Optical Networks

2.1 Introduction

Nowadays, translucent optical networks are envisioned as one of the most practical solutions to overcome the limitation of optical reach in transparent optical networks, constrained by possible physical layer impairments including both linear and nonlinear effects [29]. Optical reach refers to the distance that an optical signal can travel before its quality degrades to a level that requires regeneration. One crucial task in translucent optical network design is to strategically place the expensive regeneration resource, so as to fulfil the system requirements. As shown in section 1.1.2, there are three types of mainstream translucent architecture, namely, island of transparency, sparsely placed regeneration sites and selective regeneration [30], each with its unique property.

Under the sparsely placed regeneration sites architecture, extensive study has been conducted in terms of regeneration site placement number minimization, usually referred as regeneration node placement problem. In [5], Yang and Ramamurthy presented the detailed node structure with regeneration capability, and then proposes several heuristic such as “nodal degree first,” “centered node first,” etc, to allocate regeneration sites, specifically for the network cases with topological information only and more information on forecast traffic information. On the other hand,

researchers in [31] tried to maximize the transparency benefit of the optical networks by modeling the regeneration placement as finding the minimal connected dominating set (CDS) of a virtual graph. This award-winning solution was later verified and proved by Arunabha Sen in [7], in addition to which they proved regenerator placement problem is NP-complete. Our first contribution is based on the same architecture, where a set of nodes with the network are chosen to have regeneration capability, while the novel point of our solutions comes from the idea to use more than one optical modulation formats in the underlying transmission system. We show that by careful design, substantial capital cost can be saved, under two different investigation scenarios. There are several papers talking about using multiple modulation formats to serve mixed line rate requests in transparent optical networks [32-33], and to the best of our knowledge, it is the first attempt in translucent optical network design.

As for the selective regeneration architecture, advocated by the carriers, not much work is done in this area. The authors of [34] proposed an algorithm that deals with translucent network design under static traffic pattern. This approach deployed a regenerator for a demand at any intermediate node along its route, if necessary. Their aim was to minimize the number of rejected demands as well as the number of required regenerators. Shen proposed an efficient heuristic by grabbing the neck of the light-path method in [8] to deal with the traffic grooming problem where a set of low-bit-rate requests needed to be satisfied by the high-bit-rate light-path, with regenerator placement for each demand, if necessary. Motivated by the lack of study

under this architecture, we have proposed two efficient graph-aided solutions for two different problems, provided by the telecommunication industry. One is named as multiplexing optimization since we tackle the similar traffic grooming problem in [8] in more elegant way, while for the other problem, we build an auxiliary graph to integrate the regenerator placement and wavelength assignment tasks so that the overall number of regenerators is reduced.

The remainder of this chapter is organized as follows. In Section 2.2, the two-step planning algorithm and ILP formulation employing two modulation formats together with their corresponding illustrate examples under sparsely placed regeneration sites architecture is presented. In Section 2.3, a graph-based solution for traffic grooming optimization problem, and an integrated regenerator placement and wavelength assignment scheme by building an auxiliary graph, both of which are under the selective regeneration architecture in translucent optical networks, are presented. Section 2.4 summarizes the chapter.

2.2 Translucent Optical Network Planning with Heterogeneous Modulation Formats

2.2.1 Motivation and Problem Statements

In a translucent optical network [1], several regeneration capable nodes are strategically placed in the network, so as to assure the traffic requests can reach their respective destinations with accepted quality. Optical reach refers to the distance that an optical signal can travel before its quality degrades to a level that requires

regeneration. It is often limited by the physical layer impairments in the optical transmission links. In view of optical transmission, the modulation format of the optical signal has significant impact on the achievable optical reach [35-36]. Generally, the larger the optical reach, the more expensive the corresponding transceiver[35]. With intrinsic property of heterogeneous route distances in most optical networks, more than one modulation formats for the optical signals may be employed for different links, so as to optimize the optical reach requirement for different traffic requests, and thus reduces the number of required regeneration nodes. In this section, we propose a novel network planning architecture and algorithm to reduce the network cost in a translucent optical network by employed non-return-to-zero (NRZ) and carrier -suppressed- return-to-zero (CS-RZ) formats for optical signals running on different routes, as these two modulation formats are suggested in [35] for 40Gb/s systems. Our results show that it is a cost effective design for future backbone network planning. Please note that the heterogeneous modulation formats considered are not restricted to NRZ and CS-RZ for our algorithm. All other feasible advanced modulation formats can be taken into consideration at the network planning stage.

Node Architecture and Network Model

A typical optical regeneration node comprises a core optical cross-connect (OXC) module, a number of optical transceivers and a 3R electronic regeneration card[5]. NRZ node and CS-RZ node have similar architectures as the optical regeneration node, except that there is no regeneration card and are incorporated with different

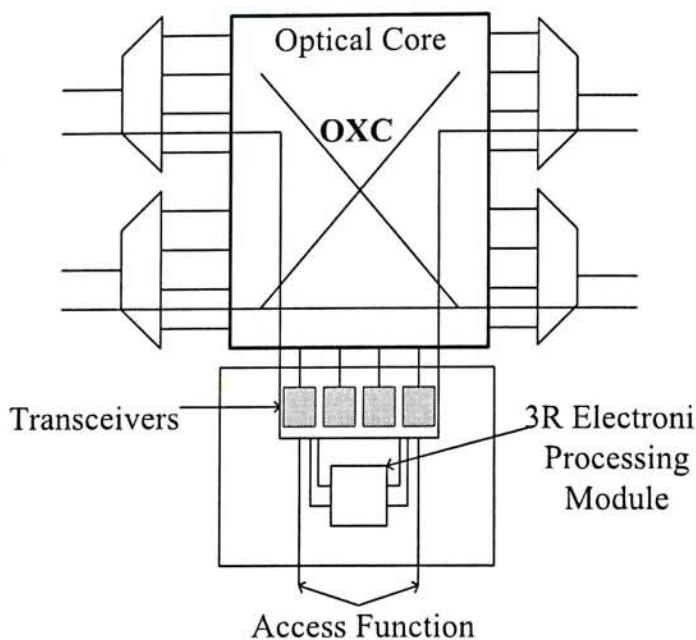


Fig. 2.1: Regeneration node Architecture

type of transceivers. Shown in Fig. 2.1, at each node, the wavelengths on the incoming fiber links are de-multiplexed and switched by the core OXC switching module, before being multiplexed onto the outgoing fiber links. For a NRZ or CS-RZ node, there are N transceiver pairs. Moreover, we

assume that M regenerator cards are equipped at each optical regeneration node in the 3R electronic regeneration module. The number of transceivers and regenerator cards in different types of network nodes is listed in Table I. Each regeneration node can receive and transmit both NRZ and CS-RZ signals. As the CS-RZ signals are generated by carving the pulses from the NRZ signals using an additional optical modulator and both of them use P-I-N photodiodes as the receiver, NRZ nodes and CS-RZ nodes can communicate with each other without any format conversion.

TABLE I NUMBER OF TRANSCEIVERS IN NRZ / CS-RZ / REGENERATION NODES

	NRZ Transceiver	CS-RZ Transceiver	Regenerator Card
NRZ node	N	-	-
CS-RZ node	-	N	-
Regeneration node	N	N	M

2.2.2 A Two-Step Planning Algorithm Using Two Modulation Formats to Realize Any-to-Any Topology Connectivity

In this section, we describe a two-step algorithm to place regeneration nodes, NRZ and CS-RZ nodes, in the network. To simplify the model, we use physical distance to represent the physical impairments accumulated along the route. More specific physical impairments evaluation model could be used like amplifier noise as the metrics. Note that the major constraint of our design is to make sure every node pair could establish at least one physical impairment feasible connection between them. That is so called any-to-any topology connectivity.

In general, the first step of the algorithm does basic preprocessing and computing while the second step is implemented to select the optimal planning map consisting of regeneration nodes, NRZ nodes and CS-RZ nodes.

Input: $G(V,E)$, an undirected graph representing the network topology. Each link consists of a pair of fibers in opposite direction. R_{NRZ} and R_{CS} denote the optical reach of NRZ and CS-RZ modulation formats.

Step 1:

Step1.1: Use Dijkstra algorithm to get the shortest path between each node pair.

Record the result in a matrix $[L_{sd}]$. This matrix will be used to justify whether a physical impairment feasible path exists between a node pair in the following steps.

Step1.2: If only NRZ modulation format (R_{NRZ}) is employed, find the minimum

number of regeneration node required to make sure that at least one feasible path exists between each node pair, denoted as m . This step is to find the minimum connected dominating set of $G(V,E)$ if the optical reach is R_{NRZ} [5].

Step1.3: If only CS-RZ modulation format (R_{CS}) is employed, find the minimum number of regeneration nodes, denoted as n , required to make sure that at least one physical impairment feasible path between each node pair. This step is similar with step2. We assume that $R_{CS} > R_{NRZ}$ and the difference is large enough to make $n < m$.

Step 2:

Step2.1: Initialize $i=m-1$. If there are i regeneration nodes in the network, denoted as regeneration node set $Set(R)$, where $n \leq i \leq m-1$, find all the possible combinations of $Set(R)$ subject to the following constraints:

Constraint 1 For each node pair in $Set(R)$, at least one feasible path exists with optical reach R_{CS} . As in our model, every regeneration node has CS-RZ transceivers.

Constraint 2 For nodes that are not in $Set(R)$, denoted as $Set(T)$, there is at least one feasible path within R_{CS} from each of them to at least one node in $Set(R)$.

For each combination, pick out those nodes in $Set(T)$ of which the physical distances to each node in $Set(R)$ are greater than R_{NRZ} , denoted as P type node. Get the number of P type nodes for each combination and record those combinations with the least number of P type node. Note that a P type node

will become CS-RZ node and the rest nodes are NRZ nodes. The aim of this step is to find the node planning map with minimum overall network cost comprises the costs of regeneration nodes, NRZ nodes and CS-RZ nodes if there are i regeneration nodes. $i=i-1$; if $i \geq n$, go to Step 4; else, go to Step 5.

Step 2.2: Given the cost of NRZ transceiver (C_{NRZ}), CS-RZ transceiver (C_{CS-RZ}) and regenerator card (C_{RE}), get the minimum normalized overall network cost of those placement maps from Step 4 for each i .

Output: The regeneration node set $Set(R)$, the NRZ node set $Set(NRZ)$, the CS-RZ node set $Set(CS-RZ)$.

2.2.3 Illustrative Examples

Our design is applied on two network topologies, namely NSFNET (see Fig. 2.2) and Pacific Bell Network (see Fig. 2.3), where all link lengths are in the unit of km. In our test, $N=M=4$. The values of M and N make no difference to the test conclusion. Since transmission of 40 DWDM channels over 1,700 km of SSMF using the CS-RZ format [35] has been demonstrated, considering that the sensitivity of CS-RZ has 1-2 dB improvement compared to NRZ, the optical reaches of CS-RZ and NRZ in 40-Gb/s are assumed to be 1700 km [35] and 1140 km (the maximum link length of the NSFNET topology and in the 1-2dB), respectively. The cost of the conventional NRZ transceiver is normalized to a value of 1, while the relative costs of a regenerator card and a CS-RZ transceiver are assumed to be higher than NRZ transceiver [36]. Table II lists the network node map of the heterogeneous-format (or

hybrid) design in the two topologies, using our proposed algorithm, as discuss in section 2.2.2. Fig. 2.4 and Fig. 2.5 illustrate the final node map from Table II.

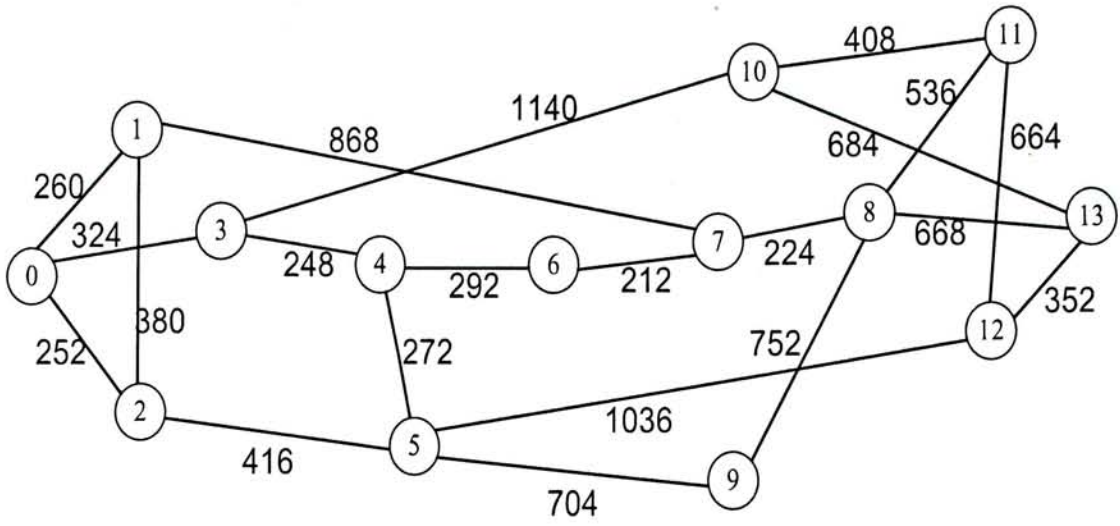


Fig. 2.2: 14-node 21-links NSFNET (Link lengths are in the unit of km)

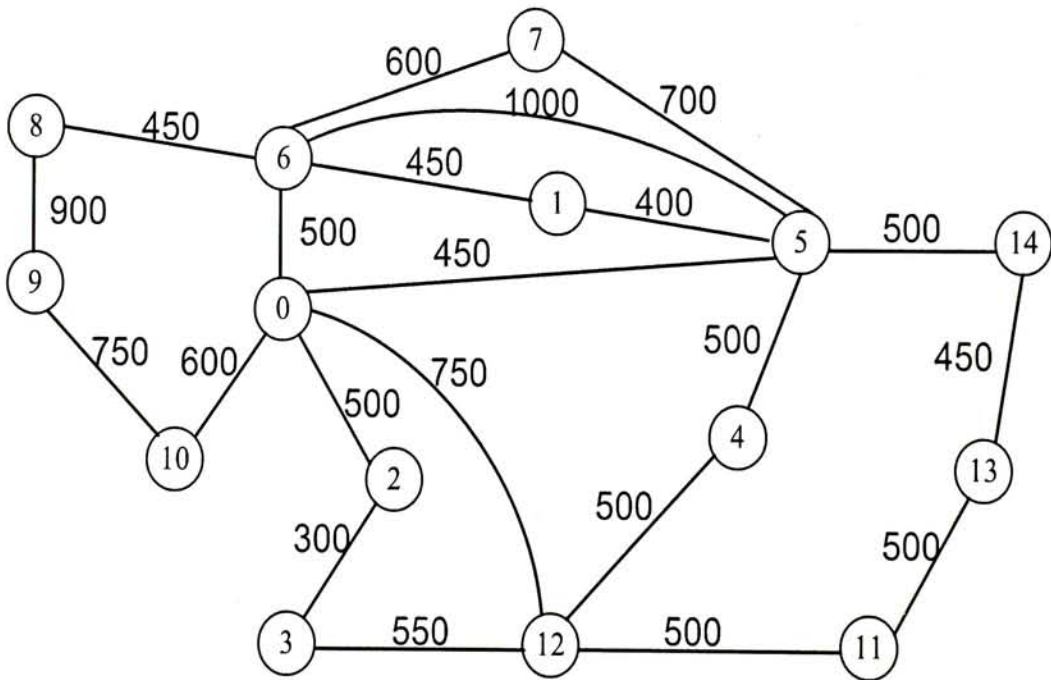


Fig. 2.3: 15-node 21-links Pacific Bell Network (Link lengths are in the unit of km)

	Regeneration node	CS-RZ node
NSFNET	8	0, 2
Pacific Bell Network	0	9, 11, 13

With this heterogeneous-format design, the relative network cost savings are estimated, as compared to the network designs with all NRZ nodes and with all CS-RZ nodes. Considering NSFNET, it is found that relative cost savings of 10%

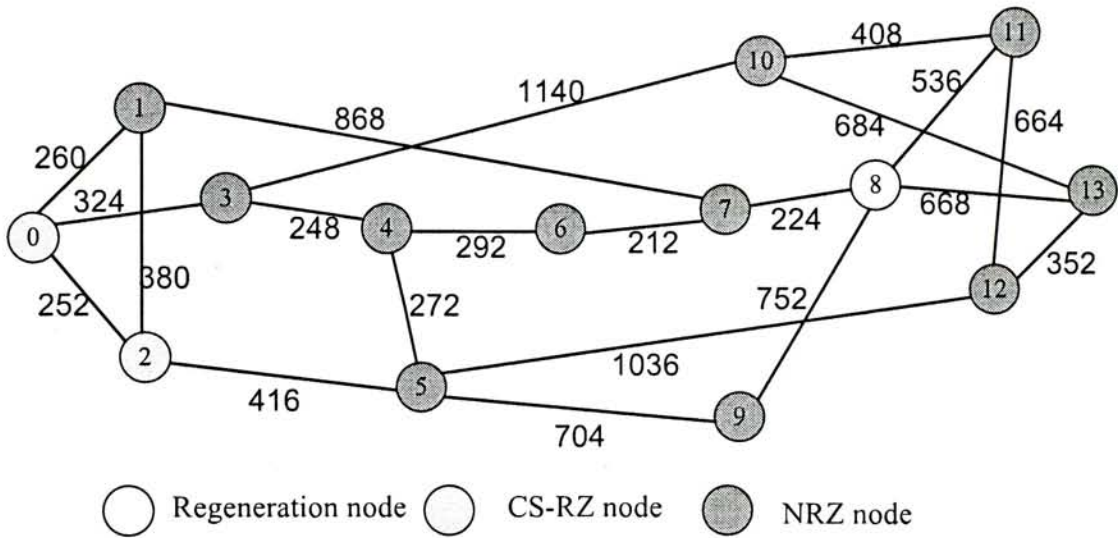


Fig. 2.4: The node map of applying the two-step planning algorithm over NSFNET network

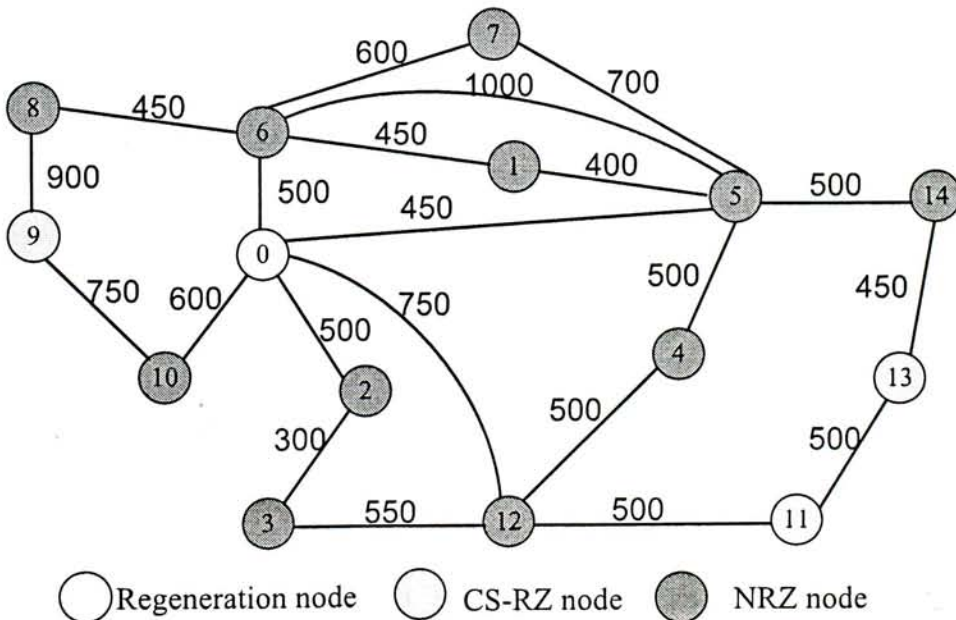


Fig. 2.5: The node map of applying the two-step planning algorithm over Pacific Bell network

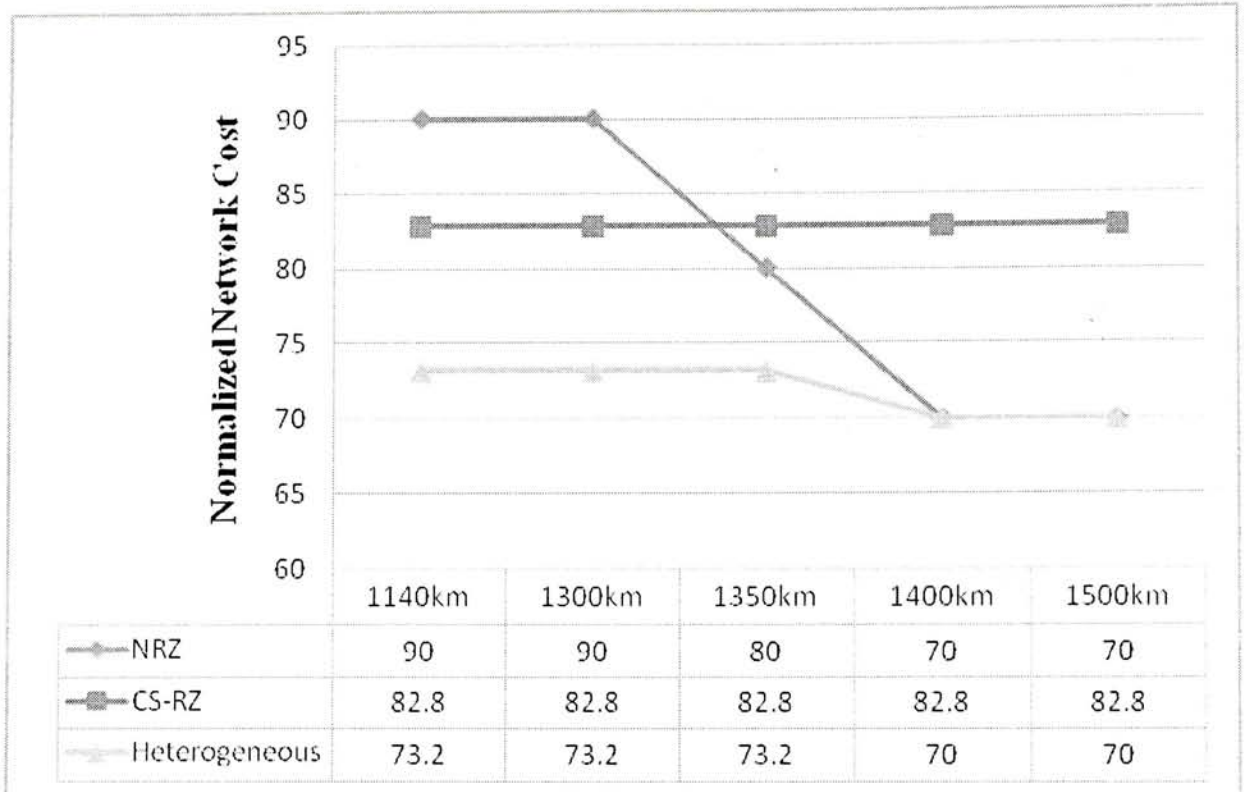


Fig. 2.6: Normalized network cost of Pacific Bell Network with different network designs, under different assumed optical reach values of the NRZ format

and 12.3% are achieved, as compared to the cases of all NRZ nodes and all CS-RZ nodes, respectively, under the assumption that the cost of a regenerator card and cost of CS-RZ transmitter are 1.5 and 1.2, with respect to the normalized cost 1 of NRZ transmitter. Similarly, for Pacific Bell Network, the respective relative cost savings are 18.7% and 11.6%.

Besides, the difference in the optical reach of the two chosen modulation formats also has significant impact on the heterogeneous-format design. For example, if the assumed optical reach value of NRZ format is varied from 1140 km to 1500 km, while that of CS-RZ format remains unchanged (1700 km), the normalized network cost of Pacific Bell Network under different design varies, as depicted in Fig. 2.6. As the optical reach of NRZ format is getting closer to that of CS-RZ format, the

advantage of using heterogeneous-format design starts to lose, due to the reduced optical reach difference and the relatively lower cost of the NRZ nodes. From Fig. 2.6, after the optical reach of NRZ format exceeds 1350 km, the network design with all NRZ nodes becomes as cost-effective as the heterogeneous-format design.

2.2.3 ILP Formulation of Minimizing Translucent Optical Network Cost with Two Modulation Formats under Static Traffic Demands

As discussed in section 1.3.1, other than ensuring any-to-any connectivity objective discussed in the last section, serving a forecast traffic matrix made up of a set of fixed light-path demands remains to be a crucial task in practical optical network planning[37]. In this part, to further illustrate our proposed heterogeneous modulation format design philosophy, we formulate an ILP tailored uniquely for the problem, specifically utilizing the two optical reaches. In the following discussion, we will first present the architecture of the regeneration site and then explain the ILP formulation in detail.

Regeneration Site Architecture

Typically, two possible 3R regeneration methods are used in the telecommunication industry[30], excluding all-optical 3R regenerator since it is still expensive and immature. One is through a pair of back-to-back transponders via a patch cable, while the other is through a dedicated regenerator card, shown in Fig. 2.7.

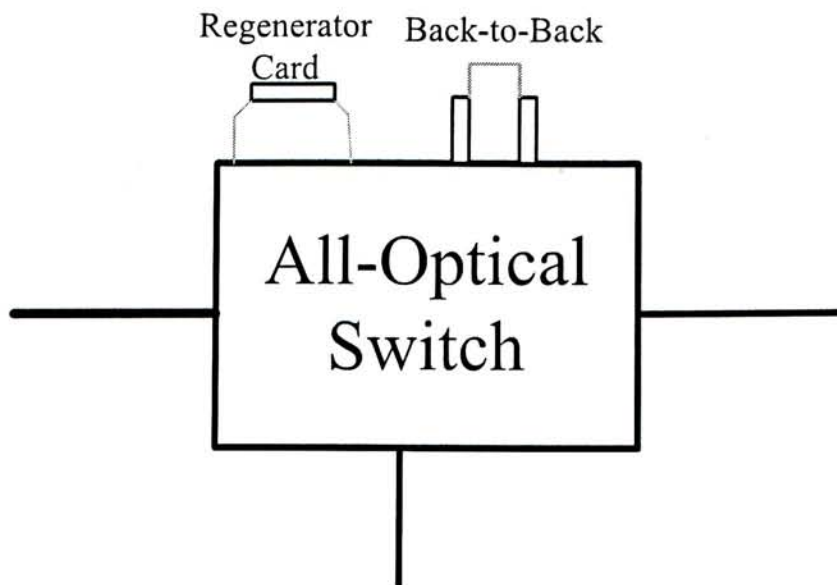


Fig. 2.7: Two 3R regeneration implementation choices

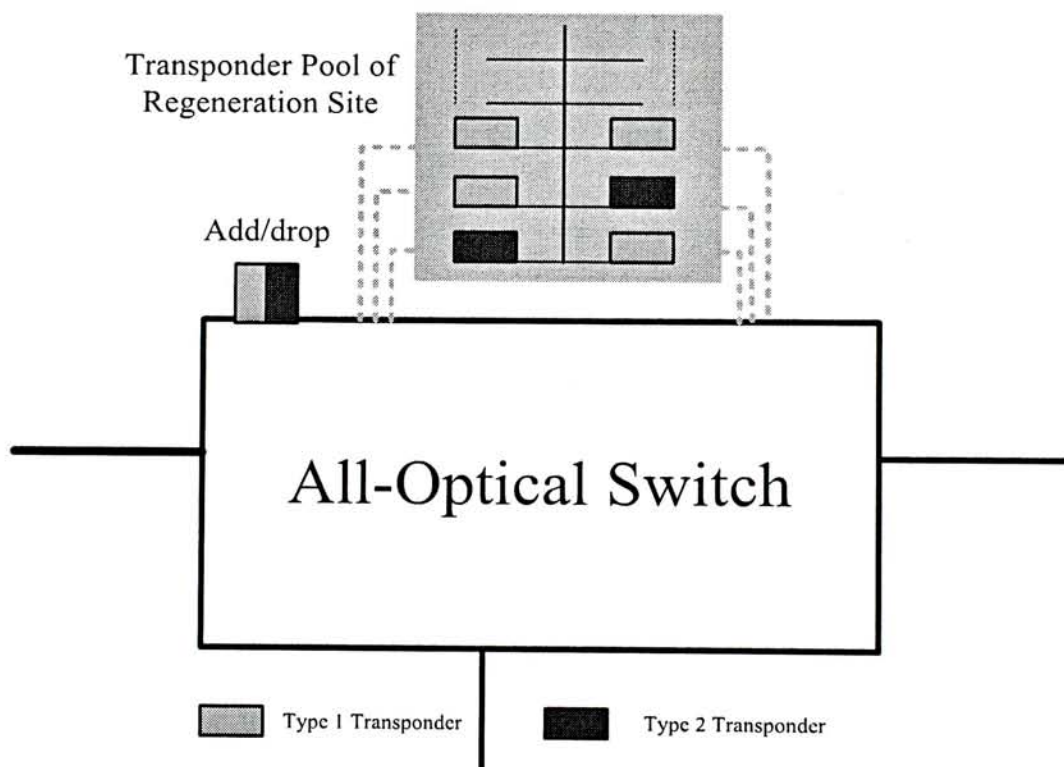


Fig. 2.8: The Regeneration Site Architecture including a pool of transponders

In our ILP formulation, we choose to use the back-to-back architecture, as it allows easier cost modelling despite the fact the regenerator card can also be used in our ILP formulation. In addition, the back-to-back architecture provides true add-drop function compared to regenerator card [30].

Our investigation is based on the sparsely placed regeneration site model, with a bundle of regeneration modules or resources. Combined with our back-to-back transponder regeneration strategy, we show in Fig. 2.8, how the transponders are arranged in the regeneration site. For those nodes selected to be regeneration site, we deploy an empty site rack at that node, with certain capacity limit. Then, if a light-path needs to be regenerated, a pair of transponders is put into one slot of the rack via back-to-back connection. As shown in Fig. 2.8, either type of transponder can be used, which could largely facilitate component management, and in turn reduce the operation cost.

ILP Formulation

The inputs of the problem are listed as follows:

- ✓ The network topology $G = (V, E)$ is given as a weighted undirected graph. V is the set of network nodes. E is the set of weighted links, with the weight representing the physical distance of the link.
- ✓ Two types of transponders, with respect to two modulation formats employed. Type 1 transponder has optical reach R_1 and cost C_1 while Type 2 owning optical reach R_2 and cost C_2 .
- ✓ The cost to deploy a regeneration site at any node is set to be C_{site} as input. This parameter is used to balance the capital cost and the operational cost, under the reasoning that the more regeneration sites maintain, the higher your operation cost.

- ✓ K is the set of static traffic demands as given.
- ✓ N denotes the maximal number of transponders that could be deployed at a regeneration site.
- ✓ Ω is the set of wavelengths in each link.
- ✓ $py(u,v)$ the link set in physical layer topology consisting the virtual link (u,v) .
- ✓ α is a constant with extremely small value.

With the network physical topology $G = (V, E)$ and optical reach R_1 and R_2 , we run the shortest path algorithm to get the distance matrix of all the node pairs in the network. With the distance matrix, we create two new virtual topologies whereas the node set V is same as that in the physical topology. In one virtual topology, if the distance of a node pair is not greater than optical reach R_1 , we create one direct edge, between this node pair, denoted as Type 1 plane. For another virtual topology, if the distance of a node pair is not greater than optical reach R_2 , we create one direct edge, between this node pair, denoted as Type 2 plane.

The variables for the ILP are defined as follows:

- ✓ Boolean variable $R(u)$ indicates whether node $u \in V$ is selected to have regeneration site.
- ✓ Integer variable $n_1(u)$ denoting the number of Type 1 transponder in node u .
- ✓ Integer variable $n_2(u)$ denoting the number of Type 2 transponder in node u .
- ✓ Boolean variable F_1^k indicates whether request k use transponder Type 1 (=1)

not (=0) at the source.

- ✓ Boolean variable F_2^k indicates whether request k use transponder Type 1(=1) or not (=0) at the destination.
- ✓ Boolean variable $f_{u,v,w}^{k,1}$ indicates whether wavelength w on the link from node u to v is occupied by request k (=1) or not (=0), in the Type 1 plane.
- ✓ Boolean variable $f_{u',v',w}^{k,2}$ indicates whether wavelength w on the link from node u' to v' is occupied by request k (=1) or not (=0), in the Type 2 plane.
- ✓ Boolean variable $f_{m,n,w}^k$ indicates whether wavelength w on the link from node m to n is occupied by request k (=1) or not (=0), in the physical topology.

The objective of the ILP is:

$$\begin{aligned} \text{Minimize: } & \sum_{u \in V} [C_{site} R(u) + C_1 n_1(u) + C_2 n_2(u)] \\ & + \sum_{k \in K} [C_2(1 - F_1^k) + C_1 F_1^k + C_2(1 - F_2^k) + C_1 F_2^k] \end{aligned} \quad (2-1)$$

Subject to:

Regeneration Site Capacity Constraint:

$$\forall u \in V, 0 \leq n_1(u) \quad (2-2)$$

$$\forall u \in V, 0 \leq n_2(u) \quad (2-3)$$

$$\forall u \in V, n_1(u) + n_2(u) \leq N \quad (2-4)$$

Commodity flow constraints:

Simply, we use $src(k)$, $dst(k)$ to denote the source node and destination node of

request k , respectively. In addition, $out(u)$ and $out(u')$ denotes the outgoing adjacent node set of u in Type 1 plane and Type 2 plane, while $int(u)$ and $int(u')$ represents the incoming adjacent node set of u in Type 1 plane and Type 2 plane, respectively.

$$\forall k \in K, s = src(k), \sum_{w \in \Omega} \sum_{v \in out(s)} f_{s,v,w}^{k,1} = F_1^k \quad (2-5)$$

$$\forall k \in K, s' = src(k), \sum_{w \in \Omega} \sum_{v' \in out(s')} f_{s',v',w}^{k,2} = 1 - F_1^k \quad (2-6)$$

$$\forall k \in K, t = dst(k), \sum_{w \in \Omega} \sum_{v \in int(t)} f_{v,t,w}^{k,1} = F_2^k \quad (2-7)$$

$$\forall k \in K, t' = dst(k), \sum_{w \in \Omega} \sum_{v' \in int(t')} f_{v',t',w}^{k,2} = 1 - F_2^k \quad (2-8)$$

$$\forall k \in K, \forall u = u' \in V (\neq src(k), \neq dst(k))$$

$$\sum_{w \in \Omega} [\sum_{v \in out(u)} f_{u,v,w}^{k,1} + \sum_{v' \in out(u')} f_{u',v',w}^{k,2}] = \sum_{w \in \Omega} [\sum_{v \in int(u)} f_{v,u,w}^{k,1} + \sum_{v' \in int(u')} f_{v',u',w}^{k,2}] \quad (2-9)$$

Virtual topology and physical topology mapping constraint:

$$\forall k \in K, \forall u \in V, \forall w \in \Omega$$

$$f_{u,v,w}^{k,1} \leq \alpha (\sum_{(m,n) \in py(u,v)} f_{m,n,w}^{k,1} - |py(u,v)|) + 1 \quad (2-10)$$

$$\forall k \in K, \forall u = u' \in V, \forall w \in \Omega$$

$$f_{u',v',w}^{k,2} \leq \alpha (\sum_{(m,n) \in py(u',v')} f_{m,n,w}^{k,2} - |py(u',v')|) + 1 \quad (2-11)$$

Wavelength usage constraints:

$$\forall k \in K, \forall m, n \in V, \forall w \in \Omega$$

$$f_{m,n,w}^k = f_{n,m,w}^k \quad (2-12)$$

$$\forall k \in K, \forall m, n \in V, \forall w \in \Omega$$

$$\sum_{k \in K} f_{m,n,w}^k \leq 1 \quad (2-13)$$

Regeneration Site Specification constraint:

$$\forall u = u' \in V (\neq \text{src}(k), \neq \text{dst}(k))$$

$$\alpha \sum_{k \in K} [\sum_{w \in \Omega} (\sum_{v \in \text{out}(u)} f_{u,v,w}^{k,1} + \sum_{v' \in \text{out}(u')} f_{u',v',w}^{k,2})] \leq R(u) \quad (2-14)$$

$$\forall u \in V (\neq \text{src}(k), \neq \text{dst}(k))$$

$$\sum_{k \in K} [\sum_{w \in \Omega} (\sum_{v \in \text{out}(u)} f_{u,v,w}^{k,1} + \sum_{v \in \text{int}(u)} f_{v,u,w}^{k,1})] = n_1(u) \quad (2-15)$$

$$\forall u = u' \in V (\neq \text{src}(k), \neq \text{dst}(k))$$

$$\sum_{k \in K} [\sum_{w \in \Omega} (\sum_{v' \in \text{out}(u')} f_{u',v',w}^{k,2} + \sum_{v' \in \text{int}(u')} f_{v',u',w}^{k,2})] = n_2(u) \quad (2-16)$$

The objective function (2-1) minimizes the total cost to serve all the light-paths in set K , consisting of the regeneration site cost and transponder cost. Specifically, the first term of the objective ($\sum_{u \in V} [C_{\text{site}} R(u) + C_1 n_1(u) + C_2 n_2(u)]$) determines the overall cost within those sparsely placed regeneration sites while the second term quantifies the necessary investment at those source and destination nodes.

- ✓ Equation (2-2) and (2-3) ensures that the number of two types of transponders at a regeneration site could not be less than zero.
- ✓ Equation (2-4) ensures that the total number of transponders allowed in a regeneration site does not exceed N .
- ✓ Equation (2-5) and (2-6) ensures either Type 1 or Type 2 transponder is used at the source node of request $k, \forall k \in K$.

- ✓ Equations (2-7) to (2-8) ensures that either Type 1 or Type 2 transponder is used at the destination node of request k , $\forall k \in K$.
- ✓ Equation (2-9) ensures that the incoming flow is the same as the outgoing flow for every node which is neither a source nor a destination of request k , $\forall k \in K$.
- ✓ Equation (2-10) ensures that the if the wavelength w of a virtual link (u,v) in Type 1 plane is used, the wavelength w on those physical links covered by (u,v) should be assigned to (u,v) ($(m, n) \in py(u, v)$).
- ✓ Equation (2-11) ensures that the if the wavelength w of a virtual link (u',v') in Type 2 plane is used, the wavelength w on those physical links covered by (u',v') should be assigned to (u',v') ($(m, n) \in py(u', v')$).
- ✓ Equation (2-12) ensures that the light-path is bidirectional.
- ✓ Equation (2-13) ensures that a particular wavelength on any link can only be used for one light-path demand at most.
- ✓ Equation (2-14) ensures that for every node which is neither a source nor a destination for a certain request, it is selected to be a regeneration site as long as the requested flow passed through it.
- ✓ (2-15) and (2-16) calculate the number of Type 1 and Type 2 transponders in each regeneration site.

2.2.4 Illustrative Numeric Examples

It is well known that ILP is time-consuming computing task. Thus, we employ a small network, specifically a six-node eight-link network [38] as shown in Fig. 2.9, with link distance attached to illustrate our formation and compare with other two cases where either one of the modulation format is used, all of which are optimal results.

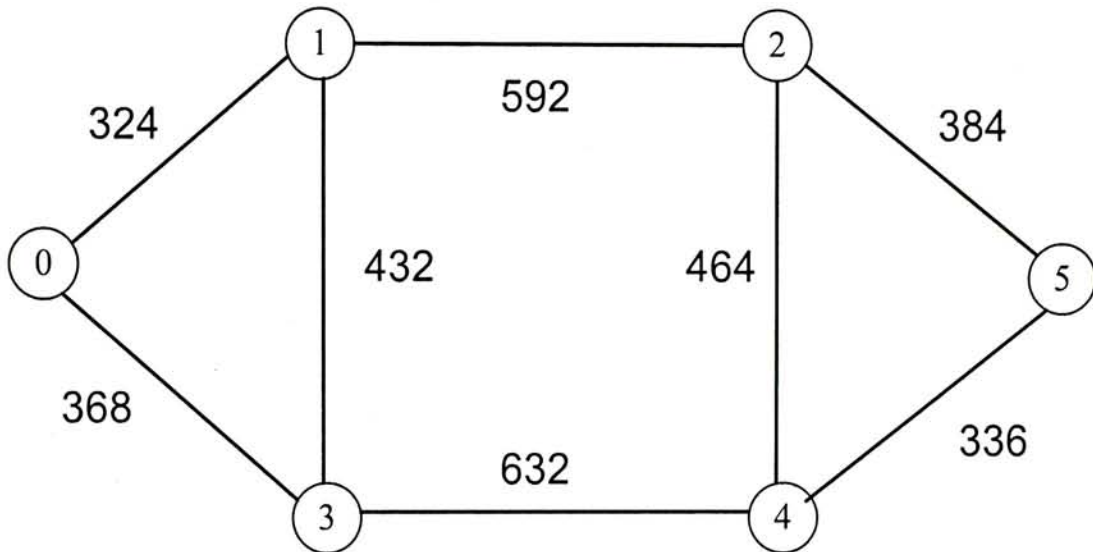


Fig. 2.9: A six-node eight-link network used for illustration

With 9 wavelengths available on each link, we set the R_1 to be the maximal link length within the network, 632km, assuming no in-line regeneration needed. For R_2 , two values, $\times 1.5$ and $\times 2.0$ of R_1 , are tested for sensitivity purpose. The traffic matrix includes 15 light-path demands, meaning that every node pair has a light-path to be established. In addition, the cost of the type 1 transponder (C_1) associated with R_1 is normalized to be 1 while type 2 transponder (C_2) has cost 1.5[36]. In order to minimize the number of regeneration sites, we tune the C_{site} to be 20.

The two simulated cases' results are shown in Table III and Table IV.

TABLE III TRANSPONDER MAP RESULT OF CASE 1

$R_1=632$ $R_2=948(\times 1.5 R_1)$ $C_1=1, C_2=1.5$	Transponder placed at source and destination		Transponder placed at each regeneration site, if any			Overall Network Cost
	Type 1	Type 2	Site Location	Type 1	Type 2	
Only type 1 transponder is used	30	-	Node 1	10	-	90
			Node 2	10	-	
Only type 2 transponder is used	-	30	Node 2	-	8	103
			Node 4	-	4	
Both of the transponder types are used	26	4	Node 2	6	2	85
			Node 4	4	0	

TABLE IV TRANSPONDER MAP RESULT OF CASE 2

$R_1=632$ $R_2=1264(\times 2.0 R_1)$ $C_1=1, C_2=1.5$	Transponder placed at source and destination		Transponder placed at each regeneration site, if any			Overall Network Cost
	Type 1	Type 2	Site Location	Type 1	Type 2	
Only type 1 transponder is used	30	-	Node 1	10	-	90
			Node 2	10	-	
Only type 2 transponder is used	-	30	Node 1	-	2	68
			-	-	-	
Both of the transponder types are used	17	13	Node 3	1	1	59
			-	-	-	

From the Table III and Table IV, the first conclusion is that heterogeneous design can always achieve cost saving compared with the other two design cases. For instance, in the second case, the savings are 13.2% and 34.4%, with respect to using Type 2 transponder and Type 1 transponder only. The reason behind this conclusion

is obvious, as heterogeneous design has more options when setting up a new connection without any penalty. In addition, based on the test results of using one optical reach with its corresponding transponder cost, 632km/90, 948km/103, 1264km/68, we derive that for a specific network, there should be an optimal optical reach and transponder cost combination that minimize the overall network cost, in accordance with the conclusion from [36], which could be a further investigation topic.

Although our proposed ILP formulation, specifically tailored for heterogeneous design under fixed traffic matrix, performs well, it is worth noting that there is also some trade off involved, if examined carefully. Recent results show that for WDM adjacent channels employing different data rates and modulation formats, the optical reach performance of each modulation format can deteriorate [39-41]. Since our design could possibly induce such situation, we argue that can be largely different. First, the study in [32] use different modulation formats for different data rates while in our case, the data rate is the same which could alleviate the penalty induced. Also, if smart wavelength assignment policy like avoiding allocating adjacent channels with different modulation formats is used, the situation can also be much better. Actually, the second method will be our next potential research direction under the same problem settings.

2.3 Resource Allocation Optimization in Translucent Optical Networks

The above two sub-problems are based on the sparsely regenerator placement design principle, receiving much research interests. In practice, the telecommunication carriers, like service providers AT&T, Verizon and Sprint in US, may model and tackle the regenerator placement problem in a different way that is named as selective regeneration, where regeneration modules or resources are placed on demand and can be put at any node[8,30]. In another saying, there is no regeneration site definition here. As mentioned before, lack of research under selective regeneration architecture has inspired us to investigate the issue from a real network operator's perspective, coupled with two important aspects, namely traffic grooming and wavelength assignment. Specifically, our contribution in this sub-chapter includes a graph based solution for traffic grooming problem and a way to constructing an auxiliary graph that integrates the wavelength assignment task into regenerator placement problem, in a selective regeneration translucent optical networks.

2.3.1 Multiplexing Optimization with Auxiliary Graph

Currently, the operational dense wavelength division multiplexing (DWDM) optical network is able to support up to 100 wavelengths per fiber and 40 Gbps per wavelength, while most connection requests are at much smaller granularities, such as 2.5 Gbps and 10 Gbps. Service providers have to install muxponders at the two ends of the wavelength path to create a multiplexing wavelength connection to

provide multiple channels per wavelength. The lower bandwidth connection requests will use these underlying channels. This is called multiplexing in DWDM networks, in the industry, referred as traffic grooming in the academics. Multiplexing optimization is to determine when and where to create 40-Gbps multiplexing wavelength connections, which is an important task for cost effective optical network planning. Most of studies in this area focus on either static traffic or dynamic traffic model [14-15]. In this study, we focus on incremental traffic model, i.e. low bandwidth connections arrive one by one and are maintained in the network for a relatively long period. This traffic model is more practical for real DWDM networks. Also, existing studies in this area seldom consider the optical layer impairments, ASE noise, dispersion, and nonlinear effects. In fact, these effects have significant impacts on the longest distance that an optical signal can travel without regeneration, denoted as optical reach, defined above already, which in turn affects the ultimate network cost [8]. In this part, we propose a novel multiplexing graph model and multiple multiplexing policies to perform low-bandwidth-connection routing and multiplexing optimization in DWDM mesh networks, combined with the incremental traffic model and physical layer constraints. Based on this graph model, we can automatically determine where to route over the network, where to use existing available multiplexing wavelength connection channels, whether/where to create new multiplexing wavelength connections, where to add regenerators, and what is the overall investment cost: all the information a planner would like to know. Clearly, it is under the selective regeneration framework. Also, the solution could be easily

extended to other cases such as 2.5G over 10G or 40G over 100G.

Problem Statement and Graph Model

In DWDM networks, a connection cost is usually modelled by two parts: optical transponder (OT) cost and common cost. The OT is an optical-electrical-optical device that is still very expensive. There are two types of OTs, named as term OT and regen OT[42], shown in Fig. 2.10. When a new wavelength connection is

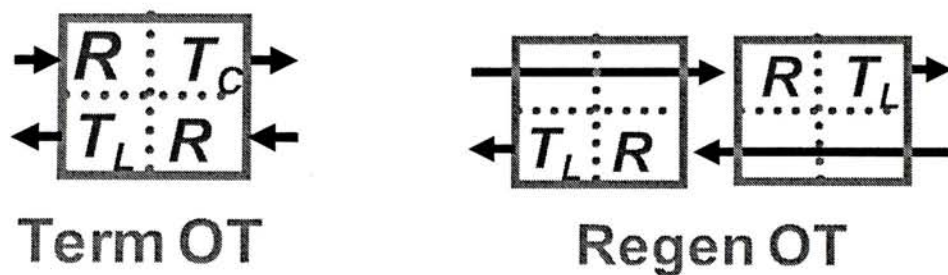


Fig. 2.10: The Structure of Term OT and Regen OT

established, a pair of term OTs is required at the two end offices of the wavelength connection. Regen OT, also referred as regenerator, is required when a wavelength connection is longer than the optical reach [42]. Typically, a pair of term OT cost more than a Regen OT. Common cost includes optical system device cost, fiber cost, optical amplifier cost, installation cost, etc., and it is averaged as cost per $\lambda_{\text{channel-mile}}$ [43]. In our multiplexing optimization problem, the objective is to minimize the overall network cost including OT cost and common cost during the lifetime of the DWDM network. For a specific low bandwidth request, there are numerous ways to provision the connection, such as establishing a new long multiplexing wavelength connection directly between source and destination, or reusing some spare channels of existing multiplexing wavelength connections

(with/without creating some new short multiplexing wavelength connections). Different decisions may affect future connections. In the incremental traffic model, we know current network status and we need to provision the new connection request without knowing future traffic. Here we propose four multiplexing policies and compare their performance. To accomplish it, we present a novel multiplexing graph model to realize different multiplexing policies by manipulating the cost of graph edges:

Step 1: With the DWDM network physical topology and optical reach, we run the shortest path algorithm to get the distance matrix of all the node pairs in the network. With the distance matrix, we create a new graph $G(V,E)$ whereas the node set V is same as that in the physical topology. If the distance of a node pair is not greater than optical reach, we create one direct edge, e , between this node pair. We set its weight $w(e)$ as one regen OT cost plus its common cost, where the common cost is calculated as its distance mileage multiplied with the per λ _channel-mile cost.

Step 2: If we need to establish new multiplexing wavelength connection between a node-pair where the distance is greater than the optical reach, the most cost-effective way is to route through the shortest path since it requires the least total regen OT cost and common cost. It is easy to verify that the cost to establish a direct multiplexing wavelength connection between a node-pair is the total path weight plus two term OT cost minus one regen OT cost. For all the node pairs with distance longer than optical reach, we find the shortest path over $G(V,E)$, then create a new edge between them and use the above adjusted path cost as its weight.

With the above the two steps, we build a full mesh graph, named as *multiplexing graph*. The weight of each edge reflects the cost to establish a direct or multiplexing wavelength connection between its end nodes.

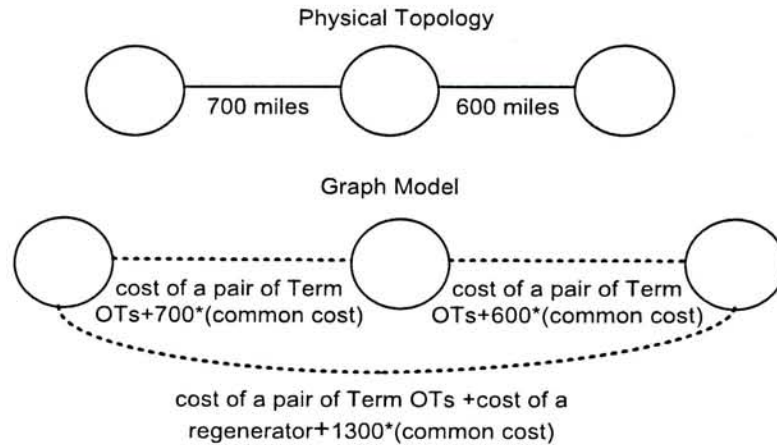


Fig. 2.11: A graph model construction example based on physical topology when optical reach is 1200 miles

To further illustrate the model building process, Fig. 2.11 shows a sample graph model construction, based on the simple linear physical topology and the 1200-mile optical reach. For simplification, we only consider 10-Gbps connections over 40-Gbps wavelengths while our model can be extended to lower bandwidth connections. Various multiplexing policies can be applied on the same multiplexing graph constructed as above. We treat each potential multiplexing wavelength connection as one link with each link having four channels and build a new graph G' (V, E') , where we create up to 4 links into E' for each edge e in E of $G(V, E)$. Then we assign different costs to those links according to following four policies and run the least cost routing to select the most cost-efficient route:

Investment cost: the first channel of a multiplexing wavelength connection is responsible for the entire wavelength connection cost and the other channels are free. The reason is that we only need OT capital investment and wavelength resource during multiplexing wavelength connection creation for the first channel request. We assign the total OT cost and common cost to a new multiplexing wavelength connection edge and zero to existing multiplexing wavelength connection edge with available channels. Such a policy tends to attract 10-Gbps connections to use existing multiplexing wavelength connection channels, no matter how long the light-path could be.

Average cost: the four channels share the multiplexing wavelength connection cost evenly. We assign one fourth of the total OT cost and common cost to each channel of the multiplexing wavelength connection including new and existing ones. Such a policy tends to encourage creating new multiplexing wavelength connections everywhere with the shortest path.

Weighted cost: the four channels share the multiplexing wavelength connection cost unevenly, e.g., with the decreasing weights such as 40:30:20:10 for the 1st, 2nd, 3rd and 4th channels. That is, we assign 40% of the total OT cost and common cost to new multiplexing wavelength connection edges, 30% or 20% or 10% of the total cost to existing multiplexing wavelength connection edges with 3 or 2 or 1 free channels, respectively. Such a policy is trying to balance the investment cost and the average cost policies.

Major-Minor cost: The previous three policies do not consider any traffic pattern. But actually, a rough traffic matrix is available and can be helpful. In this policy, we first classify network nodes as major or minor nodes. For example, we can classify the top 50% nodes in terms of total historical/forecast traffic as major nodes and others as minor nodes. The major and minor node pairs have different weight-assignment rules. For example, 35:30:20:15 for major to major edges, 60:20:10:10 for minor to minor edges, and 47.5:25:15:12.5 for major to minor edges. The basic idea is to encourage multiplexing wavelength connections between major-major node pair and discourage multiplexing wavelength connections between minor-minor node pair, to increase the possibility of low-cost multiplexing.

2.3.2 Simulation Study of Proposed Algorithm

In this section, we present the simulation results of the above four multiplexing policies in CORONET [43] topology and the corresponding traffic pattern. Note that, the traffic here refers to the wavelength service traffic only supported by a set of nodes within the topology. In the CORONET topology, there are 100 nodes globally, and 40 of them support wavelength services. For our simulation, we consider only those nodes and links within US continent, including 74 nodes, 96 links and 30 nodes with wavelength services, and 16 nodes are classified as major nodes. Also, we assume each link represents one pair of fiber between the two end nodes, and each fiber can accommodate 100 wavelengths. To evaluate the overall cost, we normalize the term OT cost, regen OT cost and common cost to be 0.75, 1 and

0.0006/ λ _channel-mile based on our study on real networks. As for the input traffic from CORONET project, we randomly generate 10-Gbps connections using CORONET traffic matrix and route them one by one under different multiplexing policies. We collect both OT cost and common cost of the four policies in three different cases, where the optical reach is set to be 1400 km, 1700 km and 2000 km, as shown in Fig. 2.12. Also, we calculate the occupancy ratio of the four policies with different optical reaches, defined as the number of channels actually used over the total channels provisioned via multiplexing wavelength connections, as shown in Fig. 2.13. Each case, we simulated 100 times and average results which is in 95% confidence interval.

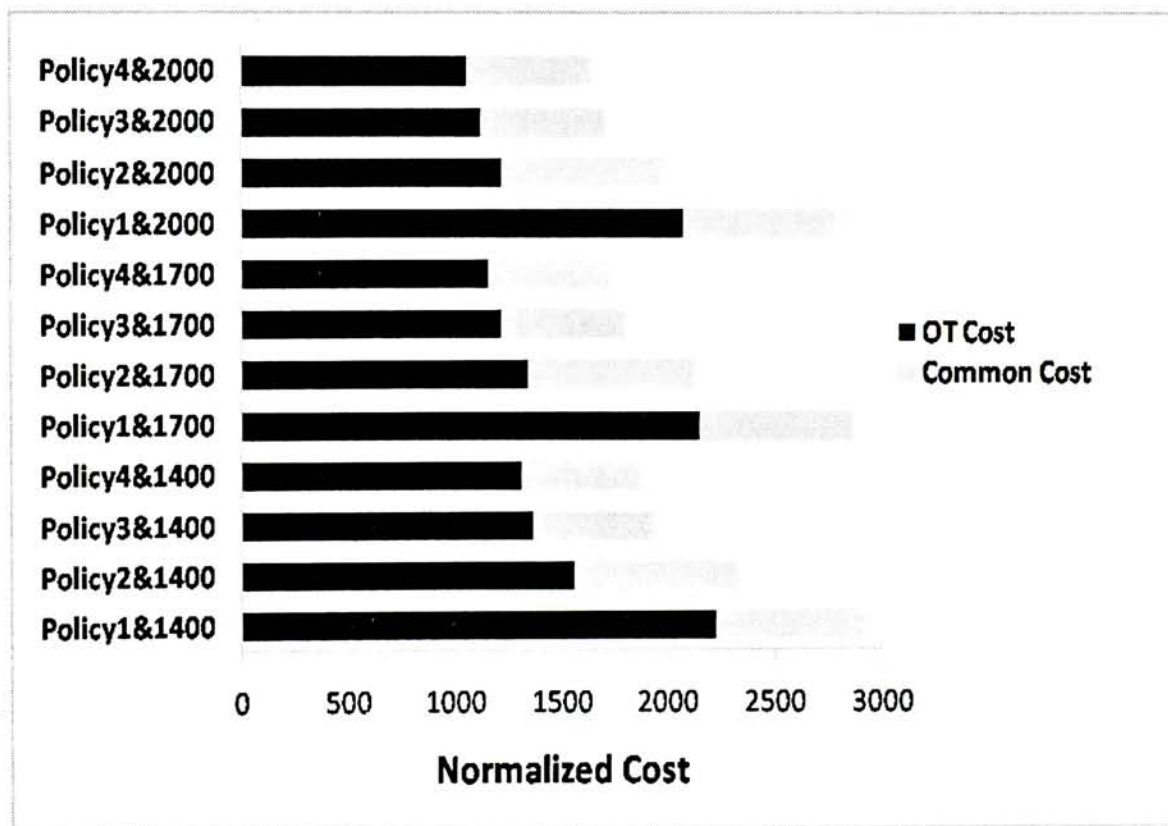


Fig. 2.12: Normalized network cost of four policies with different optical reaches

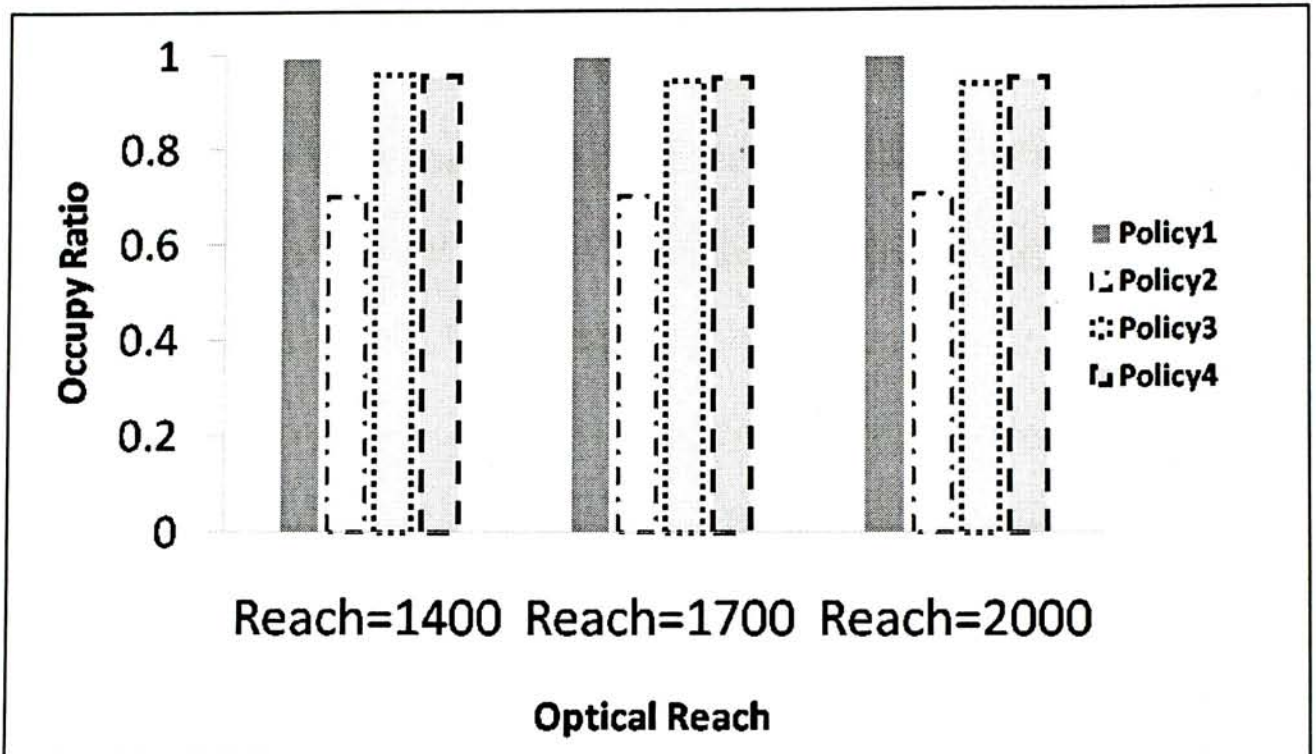


Fig. 2.13: Channel Occupy Ratio of four policies with different optical reaches

From our performance evaluation results, we noticed that both investment cost policy and average cost policy do not perform well compared with weighted cost and major-minor cost policies, shown in Fig. 2.12, since investment cost policy will route long path to use existing multiplexing wavelength connections without considering future connection requests, confirmed by the highest occupancy ratio of channels shown in Fig. 2.13. Average cost policy will try to create multiplexing wavelength connections between any two network nodes to route over shortest path. This method inevitably causes lower channel occupancy ratio, illustrated in Fig. 2.13. This policy may have smallest cost for connection request on average, but due to low occupancy ratio, the total cost is still high. Weighted cost policy is trying to make a balance between investment cost policy and average cost policy while major-minor cost

policy encourages more multiplexing wavelength connections between major-major network nodes and few multiplexing wavelength connections between minor-minor network nodes. This policy matches planners' intuition well. With the well-tuned weights for major and minor offices, it should and does outperform other policies.

The same set of multiplexing policies have been applied on to a commercial service provider's DWDM network with real traffic numbers and results in the same observation on both total cost and occupancy ratios. In fact, the major-minor cost policy has been implemented in AT&T internal optical network planning tool, named as *BIRDSEYE*.

This part deals with a complex problem that carriers are facing, routing lower speed connections over high speed DWDM networks. We have proposed a new multiplexing graph model incorporating the physical layer constraints, appeared in the form of regenerator cost in the graph model. By manipulating graph edge cost, we can easily achieve different objectives using different multiplexing heuristics. Based on this model, we have proposed several multiplexing policies and evaluate their performance using CORONET network topology and traffic as well as the real network topology and traffic. The results have shown that our proposed major-minor cost policy can provide significant network cost savings compared to other policies.

2.3.3 An Efficient Regenerator Placement and Wavelength Assignment Solution

In 2.3.2, we investigate the traffic grooming problem coupled with regenerator placement under selective regeneration architecture. In this part, we will describe another interesting problem and then present an integrated graph-based solution for it, with selective regeneration architecture assumption.

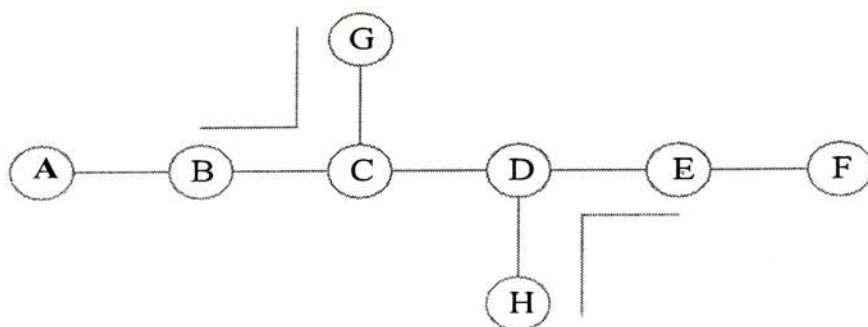
Regenerator placement and wavelength assignment (RPWA) are two major tasks during wavelength service provisioning in optical networks [19]. Regenerators are necessary but expensive. Within an optical network, a wavelength connection has to be regenerated after travelling a certain long distance (typically 1500km or longer) via an optical-electronic-optical (OEO) regenerator due to the physical impairments in fibers. This distance limit is called optical reach. Also a regenerator is required to perform wavelength conversion if there is no common free wavelength along the selected route which is called wavelength-continuous constraint. However, wavelength change at regeneration locations is not preferred, unless necessary. This is because a wavelength connection with the same wavelength at two sides of a regenerator would greatly facilitate site loop back testing, failure identification, and maintenance in field operations at the regenerator site. Thus in this study, we make the number of regenerator minimization as our first objective and the number of wavelength change minimization as our second objective.

In an optical network, a regenerator is required mainly due to either optical reach constraint or wavelength continuous constraint. As a regenerator due to optical reach

is inevitable, we can only reduce the number of regenerators due to wavelength continuous constraint. Wavelength assignment has significant impact on continuous wavelength availability. Previous studies often provide separate solutions to the RPWA problem [19]. In this study, we propose an integrated approach to this problem. Specifically, we provide a novel auxiliary graph model to combine regenerator placement and wavelength assignment together. By assigning the right cost weight to the auxiliary graph edges, we can easily decide where to place regenerators and which wavelength to select by running the least cost algorithm over the graph, such that the overall number of regenerators required is minimized.

Problem Statement

Fig. 2.14 shows a partial network with 8 ROADM (Re-configurable Optical Add-Drop Multiplexing) nodes and 7 links. Assume the optical reach is 2 hops. We have connection 1 BCG on wavelength 1, and connection 2 HDE with wavelength 1. For a new connection 3, ABCDEF, the minimal number of regenerators is 2 due to optical reach. Problem is the placement of the two regenerators and the choice of the wavelength. An intuitive algorithm would place the regenerator greedily choosing node C and node E for regenerators and wavelength 2 for the first 2 wavelength connections and wavelength 1 for third wavelength connection with first-fit wavelength assignment. This solution would leave wavelength 1 on link CD. However, a better selection would be to place the two regenerators at node C and node D, and select wavelength 2 for wavelength connections ABC and DEF, but wavelength 1 for link CD. The reason is that wavelength 1 on link CD cannot be



- Connection 1: BCG with wavelength 1
- Connection 2: HDE with wavelength 1
- Connection 3: ABCDEF with 2 hops maximal reachability

Fig. 2.14: An example of regenerator placement and wavelength assignment

expanded to any other node while wavelength 2 on link CD could be expanded to node G or node H.

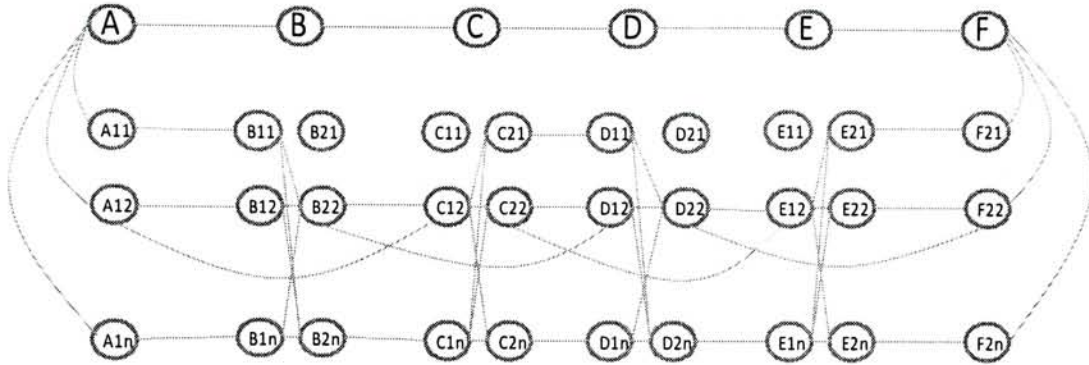
This example illustrates the basic idea of our approach:

Given an optical network topology $G(V,E)$, where V is the set of ROADM nodes and E is the set of optical links, and network status, i.e., the available wavelengths at each optical links, for a specific wavelength request $\langle \text{source}, \text{destination} \rangle$, place minimal regenerators and choose wavelength with the least wavelength fragmentation in the network.

In the following part, to cope with the requirement, we will present one auxiliary graph RPWA algorithm. By assigning proper weights on the graph edges, a shortest weight path will produce the right regenerator placement and wavelength assignment to reduce the number of regenerators needed due to wavelength continuous constraint.

Auxiliary Graph Approach

Given a graph $G(V,E)$, reachability matrix M created by *optical reach*, number of wavelengths per link w , for any circuit request (s,t) , we first find the shortest distance path as the route $R=(s,r_1, \dots, r_n, t)$. Then we construct the following auxiliary graph:



Links between two nodes have weight: regen cost
 Links inside a node have weight: $C1+C2$,
 $C1$: wavelength channel change penalty
 $C2$: wavelength fragmentation penalty

Fig. 2.15: Auxiliary graph construction example

- For node $v \in \{s,t\}$, we build w virtual nodes v^1, \dots, v^w , and one edge from v to each of the virtual nodes with edge weight 0, where w is the number of wavelengths supported in a fiber.
- For each node $v \in R \setminus \{s,t\}$, we build $2w$ virtual nodes $v^{11}, v^{21}, \dots, v^{1w}, v^{2w}$ and one edge from v^{1i} to v^{2j} with edge weight w^{ij} , where i and j range from 1 to w , and $w^{ij} = C1+C2$. Here $C1$ represents the wavelength change penalty: if i equals j , $C1$ is 0, else $C1$ is C_w ; $C2$ stands for wavelength fragment penalty: after the connection chooses wavelengths i and j on two sides of node v , we count the available degree of node v on wavelength i and wavelength j , say x^i and y^j , and then the wavelength fragment penalty function is set as: $C2=e^{1/x^i} + e^{1/y^j}$. However, if the available degree x is zero, we set the $1/x$ item as -1 . The reason is that we

reduced one wavelength fragment and the penalty value of -1 means rewarding.

The exponential function guarantees the value as positive.

- For each link $e \in E$, if e is in route R , find all feasible channels in e , $a(e)$. So for each wavelength $\lambda \in a(e)$, find the two end nodes of e , A_e and Z_e , locate the two virtual nodes $Ae^{2\lambda}$ and $Ze^{1\lambda}$ (or s^λ , t^λ if at the end of the request), and create an edge between them with weight $C_r + kw_e$, where C_r is the regenerator cost and w_e is $1/a(e)$, here $a(e)$ is the current available channels on link e , and k is a scaling factor for adjusting the relative cost of w_e to C_r . The basic idea of w_e is to encourage the usage of links with more available channels.
- Similarly for each express link $e \in M$, if e is in route R , find all available channels in e , $a(e)$. So for each wavelength $\lambda \in a(e)$, find the two end nodes of e , A_e and Z_e , locate the two virtual nodes $Ae^{2\lambda}$ and $Ze^{1\lambda}$ (or s^λ , t^λ if at the end of the request), and create an edge between them with weight $C_r + kw_e$, where C_r is the regenerator cost and w_e is $1/a(e)$, and $a(e)$ is the current available channels on link e .
- Find the shortest path from s to t . Setting $C_r \gg w_e$ and $C_r \gg w^{ij}$, the shortest path will use minimal number of regenerators, with minimal wavelength changes.

Fig. 2.15 shows the graph construction result based on the example in Fig. 2.14, where the wavelength 1 is used in link BC and link DE.

2.3.4 Simulation Study of Proposed Algorithm

In this section, we compare our proposed auxiliary graph approach two other different approaches. Please note that we simply use shortest distance path between any two nodes as selected route and thus all the three approaches are applied on the same route. By fixing the route, we are focusing on the regenerator placement and wavelength assignment only. The following is the detail description of other two approaches.

Approach 2: After finding the shortest distance path between source and destination, we first list all the regeneration node placement combination with the least regenerator number along the path, since there are probably multiple placement results having the same number of regenerators. For instance, the case in Fig. 2.14 can place regenerators at node C and E, node B and D, or node C and D, all of which needs 2 regenerators to serve the request. Then, this placement solution would choose the regenerator combination that minimizes the sum of the inverse of available wavelengths over all separated wavelength connections [19], i.e., $\min \sum 1/A(i)$, where $A(i)$ is the available wavelengths on wavelength connection i due to regenerator placement. In the above process, first-fit wavelength assignment is used to select wavelength for different segments.

Approach 3: For any specific circuit request, we first find the shortest distance path as the route. Then starting from the source node, greedily choose the farthest reachable node with available common wavelength, i.e., the distance between the selected node and source node is still within optical reach, as the next regeneration

node and also as the next starting node, until the destination node of the request is reached. In the above process, first-fit wavelength assignment is used to select wavelength for different segments. Again, we use first-fit as the wavelength assignment scheme.

We apply approach 2, approach 3 and the auxiliary graph approach (approach 1) over CORONET [43] topology, with uniform distributed traffic pattern. In the CORONET topology, there are 100 nodes globally. For our simulation, we consider only those nodes and links in US, including 74 nodes, 96 links. Also, we assume each link represents one pair of fiber between the two end nodes, with each fiber supporting 40 channels cases¹. We randomly generate wavelength service request one by one until the certain amount of requests are served. Other simulation parameters are set as follows: *optical reach* is 2000km; Wavelength change penalty C_w is set 1 while the scaling factor k is set 10; regenerator cost C_r is 800. We collect the overall number of regenerators as well as the number of wavelength changes of the three approaches with the same request arrival process. Also, we calculate the number of regenerators needed, using the placement method of approach 3 without wavelength continuous constraint, as the benchmark to get the number of regenerators for optical signal regeneration, denoted as N^{base} , thus getting the number of regenerators used for wavelength conversion of the three different policies by subtracting N^{base} from the overall number of regenerators needed for each policy. Fig. 2.16 shows the wavelength conversion regenerator number results, while Fig. 2.17 illustrates the

¹ CORONET assumes 100 channels per fiber. In this study, we use smaller fiber channel size to observe the performance.

number of wavelength change results, with different number of overall served requests. Each case, we simulated 100 times and average results which is in 95% confidence interval.

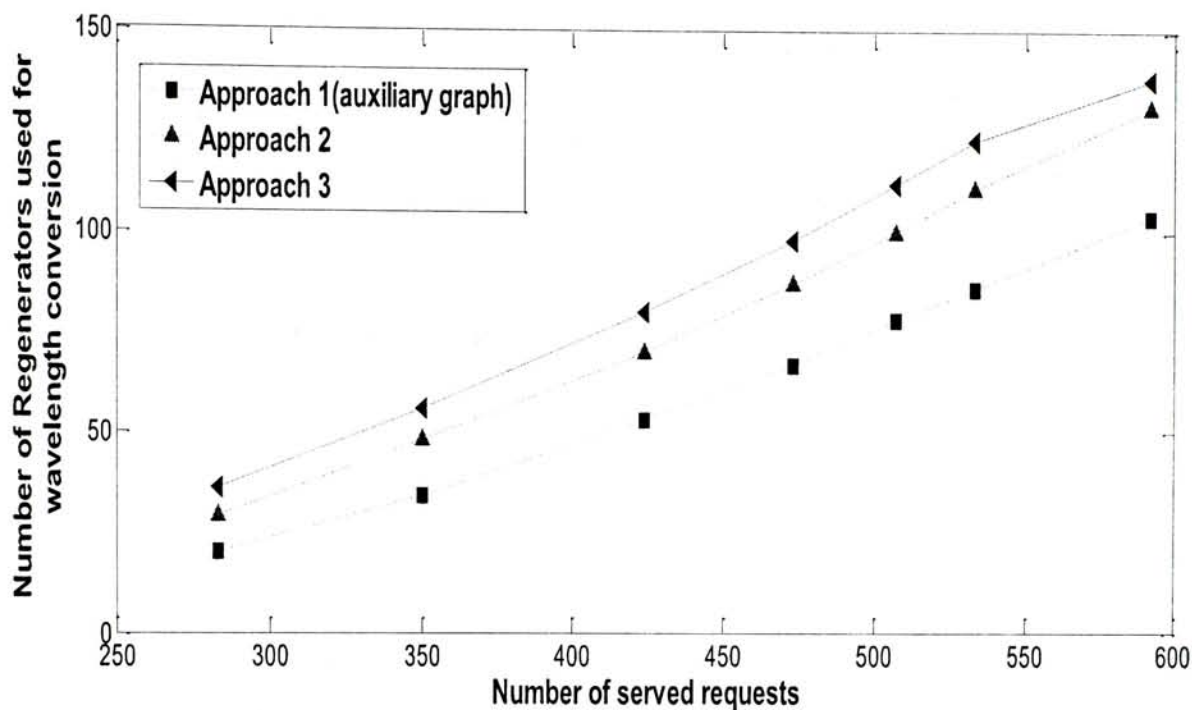


Fig. 2.16: Number of Regenerator needed due to wavelength conversion

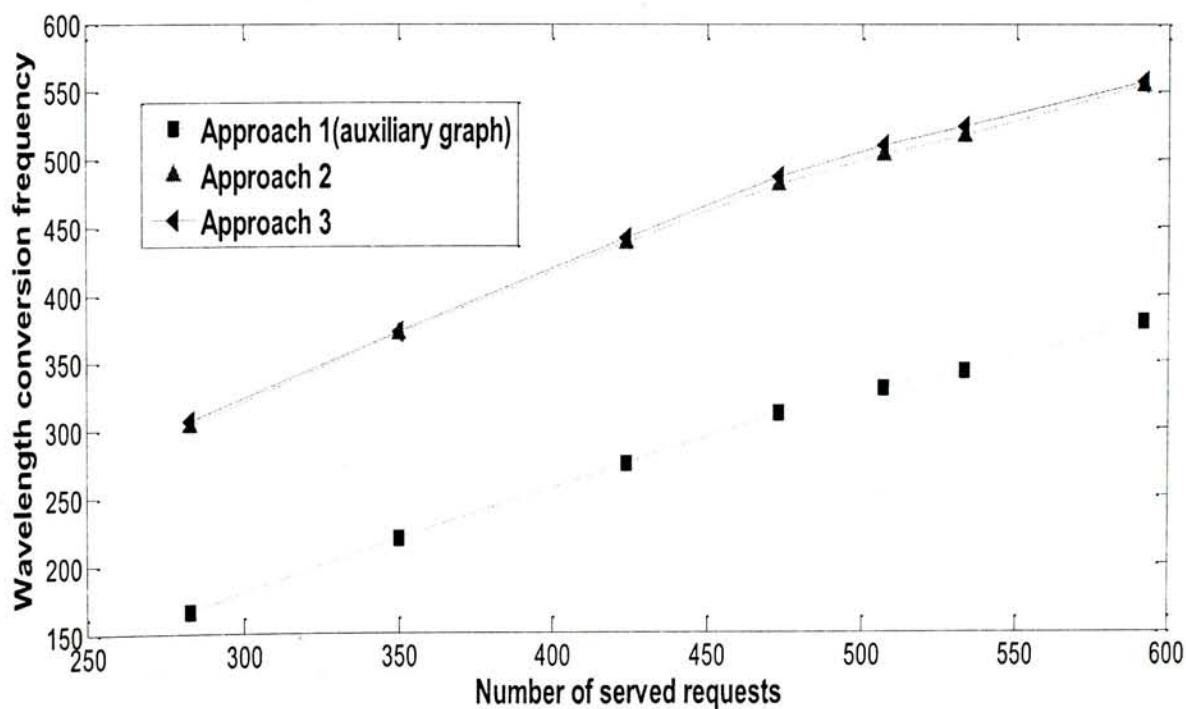


Fig. 2.17: Wavelength conversion times

From Fig. 2.16, it is easy to find that our auxiliary graph approach uses the least number of regenerators for wavelength conversion. This is mainly due to wavelength fragmentation reduction by integrating the regenerator placement and wavelength assignment together through constructing the auxiliary graph model, while the other two approaches do not provide such intelligent handling. In fact, as the network is getting more and more congested, the performance advantage becomes more significant, as a result of more wavelength fragmentation reduction possibility. On the other hand, approach 2 and approach 3, despite their simplicity, do not consider the wavelength fragmentation effect for future request, thus resulting in more regenerators needed for wavelength conversion. Furthermore, Fig. 2.17 clearly verifies our expectation that our auxiliary graph approach introduces the minimal times of wavelength change, preferred by the service provider due to field operation convenience, since we add the wavelength change penalty in the auxiliary graph.

In this part, we present a novel auxiliary graph approach to address the RPWA problem. Our basic idea is to reduce wavelength fragmentation during current regenerator placement and wavelength assignment for future request, such that the total regenerator required for wavelength conversion is minimized. Simulation results indicate that our proposed approach outperforms other common heuristics significantly. This study illustrates that we can reduce the number of regenerators required for wavelength conversion by carefully designing RPWA approach that takes future requests into consideration.

Also, the graph approach is more like a general tool in terms of potential applications

regarding the flexibility of assigning weights policies.

2.4 Summary

We have studied four sub-problems in translucent optical networks. The first two problems are based on the sparsely placed regeneration site architecture, in which we attempt to use multiple modulation formats to adapt the underlying diverse optical reach requirements. A two-step planning algorithm and an ILP are presented to deal with topology connectivity and traffic matrix serving objective, respectively, while trying to minimize the overall network cost including transponder and regeneration site cost. Additionally, we have investigated another two important problems under the selective regeneration architecture in translucent optical networks with graph-based solutions. For the multiplexing optimization problem, we have showed the way to build a decision making graph over which different multiplexing policies can be easily applied together with regenerator placement and wavelength assignment task. Then a new optimization opportunity is identified by combining the regenerator placement and wavelength assignment task together into a auxiliary graph, through which both the number of regenerators needed for wavelength conversion and the wavelength conversion frequency are largely reduced. Other than the problems themselves, we believe that we have demonstrated the possibility and usefulness of applying decision making graph approach in optical network planning research area, which could be used as a common method to solve such problems.

Chapter 3 Adaptive Fault Monitoring in All-Optical Networks Utilizing Real-Time Data Traffic

As mentioned in the abstract, in this chapter we propose a novel fault detection and localization scheme for all-optical networks with the information of real-time data traffic. Our adaptive fault localization framework is based on combining passive and proactive monitoring solutions, together with adaptive management in two phases. Numerical results indicate that our proposed scheme has good scalability, in terms of the number of fault monitors required. Also, we show that our framework allows more flexible network design, and requires much less monitoring bandwidth when compared with the passive monitoring solutions.

3.1 Introduction

Owing to the tremendous bandwidth demand of Internet traffic, optical fiber, with its vast transmission capacity, is the only promising transmission medium for backbone networks. With the recent development of optical fiber transmission technology and wavelength division multiplexing (WDM) technique, reduction in optical component cost, as well as the transparency to diverse modulation formats and protocols, has enhanced the feasibility and practicality of all-optical networks [44]. Nevertheless, all-optical networks are vulnerable to physical failures, such as fiber cut, optical cross-connect (OXC) malfunction and optical amplifier breakdown [29]. Due to the extremely large transmission capacity of all-optical networks, these possible failures

may be translated to disastrous communication disruption. Hence, fault management is one of the crucial aspects in network management to assure network reliability and availability. With the increased complexity of the network topology, fault detection and localization may incur significant management and operating costs. Thus, an efficient and cost-effective fault detection and localization system is highly desirable to assure the specified levels of quality of service [45]. In this paper, we propose a novel adaptive fault monitoring framework to fulfill these requirements in all-optical networks.

In all-optical networks, fault localization is more complicated than that in opaque networks as the impact of a single fault may propagate without electronic boundary. Until recently, there have been two major solutions to monitor link failures in all-optical networks, namely passive detection and localization [25], as well as proactive detection and localization [21]. Passive monitoring solution places equipment called monitor to collect fault alarms over the whole network and localize the failure according to the alarms received from all monitors. Link-based monitoring is the most straightforward and conventional passive monitoring solution that requires one monitor per link. To reduce the number of monitors, the concept of monitoring cycle (m-cycle) [24] has been introduced. However, as the network topology is becoming more complex, much effort has to be made to design a feasible m-cycle coverage solution. Furthermore, even if a feasible cycle set is found, the cost of the required monitors is quite substantial. Besides, the extra monitoring bandwidth cost is also getting high, as each monitoring cycle requires one distinct wavelength in

an all-optical WDM network. On the other hand, the authors in [21] have proposed an efficient failure detection and localization scheme by sending out a series of proactive probes with perfect feedback. The idea behind proactive detection is to fully utilize the unique property of all-optical light-path. In other words, one light-path could detect a number of consecutive fiber links simultaneously, if no failure is incurred. With the proactive monitoring scheme, it has been proved that the probing effort can achieve approximately the entropy of the network state under the probability link failure model assumption, in terms of information theory. Nevertheless, this proactive monitoring scheme may not be practical to be employed in practical transparent optical networks. First, this proactive probing scheme can only be applied to Eulerian networks, each of which contains an Euler trail (a path containing all the links without repetition). Although the authors in [21] have further improved their scheme to accommodate node failures and have demonstrated that all network topologies could be transformed to Eulerian networks, it is still unrealistic to configure the switching nodes to meet the requirements, as it may disrupt the existing connections and may largely increase the management cost. Besides, the requirement on the probing time and frequency is still not yet resolved.

Motivated by the pros and cons of both passive and proactive detection solutions, we have developed a novel fault detection and localization framework that utilizes the concept of adaptive network management. Compared with the passive monitoring solutions, our proposed adaptive solution requires fewer monitors and incurs minimal bandwidth cost. Meanwhile, our framework is complete and practical, when

compared with the proactive monitoring scheme in [21]. In general, our framework makes use of the real-time network traffic, whose routes are flexible to form the real monitoring trails, to passively monitor the network link states, and then proactively sends probes to detect more link states according the passive monitoring result.

3.2 Adaptive Fault Monitoring

3.2.1 System Framework

In this section, we introduce the concept and architecture of our adaptive fault monitoring scheme for all-optical networks. Single link failure is assumed in this work, as it is the dominant scenario, and a link between two nodes represents a single fiber supporting bidirectional transmission. The framework will still work for the case of unidirectional transmissions, only with doubled number of links to be monitored. In principle, it is possible to include multiple concurrent failures monitoring capability into our scheme, however bringing higher system complexity.

In our system, a central control facility, which maintains the network resource information in a database, is assumed to be responsible for client request collection, routing path computation, light-path establishment by parallely configuring the corresponding OXCs along the selected path, as well as failure detection and recovery. To achieve all these functions, a separated control plane is necessary. It can be implemented with either out of fiber configuration or in-fiber configuration, such as a dedicated wavelength channel. From the reliability point of view [46], it is more reasonable to adopt the out-of-fiber configuration, rather than the in-fiber

configuration. For instance, the out-of-fiber configuration allows us to use different schemes to assure survivability, while the in-fiber configuration protection scheme should design mechanisms combining the data plane and the control plane. Besides, the out-of-fiber configuration supports the separation of the control plane and the data plane, which is crucial for maintaining network operation properly, in case of any failure in the data plane. In this work, we design a novel mechanism to perform fault localization in an all-optical network architecture consisting of physically separated data and control planes, in which we try to minimize the capital cost to monitor the data plane network link state by fully utilizing the separated data plane and control plane architecture, combined with real-time data traffic.

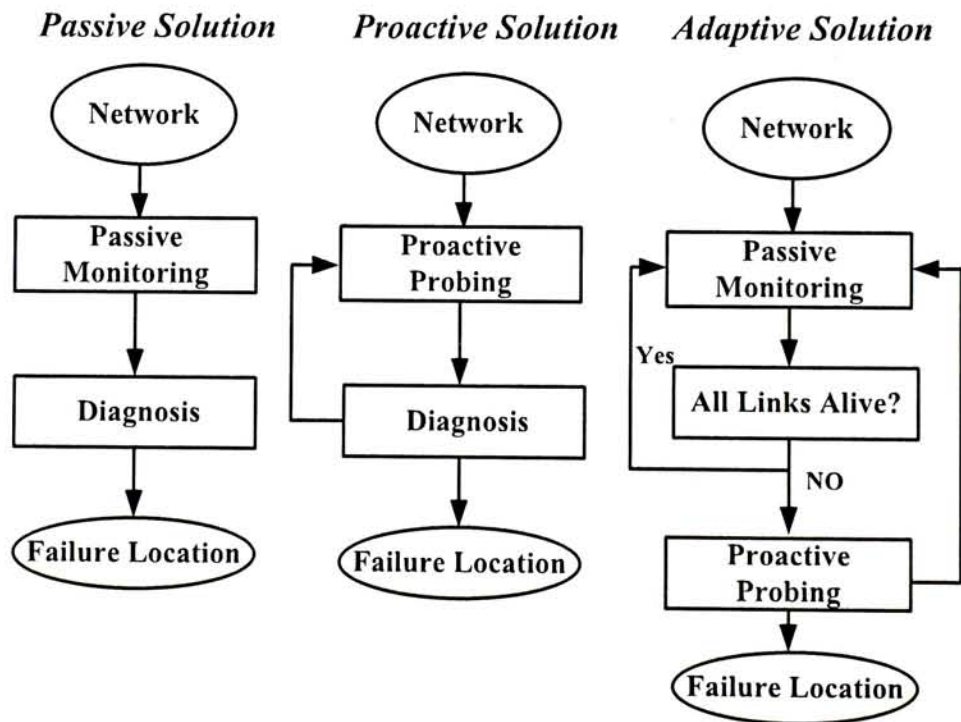


Fig. 3.1 Fault monitoring solutions: passive, proactive, and adaptive

Fig. 3.1 shows the basic idea of our scheme, comparing with both passive and proactive monitoring solutions. The overall process of our scheme comprises two phases. The first phase (Phase 1) is passive monitoring. One special feature of our

passive monitoring system is to send passive monitoring probes according to the data plane traffic condition and its routing method. Hence, the collected link state information (alive or failed) in the whole network merely depends on the previous traffic condition and its routing method, without any interruption to the data traffic. This feature will be further discussed in the later sections. After a short period of time, the network management plane checks all the received link state information and makes decision whether it is necessary to execute Phase 2. If Phase 2 is executed, the management plane triggers the designated source nodes to send probes to certain destination nodes so as to estimate the exact location of the failed link. In general, as one light-path may be disrupted by a few possible fiber cuts in an all-optical network, Phase 1 aims to narrow down and sort out the possible failed links, while Phase 2 can further determine the actual location of the failure.

3.2.2 Phase 1: Passive Monitoring

The fault monitoring framework discussed in the previous section can be realized by a novel technique, namely label tracing monitoring (LTM). Ideally, there are three components in a LTM system: Label Source (LS), Link Label (LL) and Label Monitor (LM). LS injects link labels into the network, while different LLs are designed to denote different links in the network. LM is placed to gather labels in order to retrieve link state information. Fig. 3.2 is a simple example to illustrate how these three components function. Each LS is capable of generating a path label (PL) that contains the all link labels from source to destination in a light-path. As shown in

Fig. 3.2, a light-path LP1 is to be established from LS1 to LS3. The central control facility receives such request and configures the corresponding OXCs. It further asks LS1 to embed a path label (a,b,c) into the real time data traffic. This path label will be detected only at the LMs along the path, if any. In this example, the path label (a,b,c) is received at the LM. As this label is detected at the end of link b, the system can only retrieve information that links a and b are alive (denoted as a^* and b^*), since the labels in a path label is ordered. Similarly, if another light-path LP2 is set up from LS3 to LS2, only label c can be retrieved at the LM (denoted as c^*). If these two light-paths are set up simultaneously, labels a^* , b^* and c^* will all be received at the LM, which indicates that no link failure happens. This procedure is regarded as Phase 1. It is passive, as no pre-designed probing scheme is involved. The probes are sent according to the traffic pattern, which makes control cost low. The goal for Phase 1 is to fully utilize the randomness of the real traffic and thus reduces the management cost.

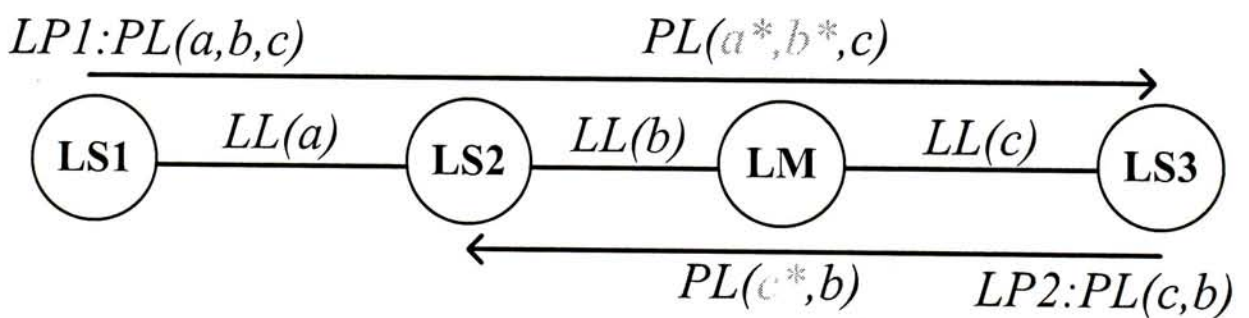


Fig. 3.2: An example to illustrate the label tracing monitoring (LTM) system

3.2.3 Phase 2: Proactive Probing

At a certain time checkpoint, the system will check the label information received at

the LMs. If all link labels in the whole network are collected, it means all links are alive and thus Phase 2 will not be executed. Phase 2 is executed if there are one or more link labels missing.

As stated before, Phase 2 proactive probing is based on the result of the Phase 1. To avoid any disturbance to the data plane traffic, Phase 2 proactive probing tries to utilize the free wavelength resource in the network to do the link fault diagnosis. In other words, with the available wavelength resource, a set of LM locations and the missing link labels at the LM after Phase 1, a feasible probing algorithm is executed to detect the states of those links with missing link labels.

First of all, we introduce a graph model commonly used in traffic grooming problem to represent the available wavelength resource in the whole network. The graph model has W planes, where W is the number of wavelengths supported by the network. Each plane, denoted as $G_\lambda(V_\lambda, E_\lambda)$, corresponds to a particular wavelength λ and the nodes, V_λ , in each plane correspond to the nodes in the physical topology. In each plane, there is an edge, E_λ , between two nodes if a fiber link exists between the two nodes, and the relative wavelength is free in that fiber link. With this graph model information, we design a heuristic for network diagnosis. The basic idea is trying to find a set of proactive trails that could uniquely identify fault that may happen to those links with missing link labels after Phase 1, by observing the instant link labels at LMs. The proactive trail formation rule is similar to that in [47]. In our algorithm, a *trail*, which denotes a light-path, ends at a certain LM on a particular wavelength plane. Nevertheless, due to the limited wavelength resource,

there may not be enough trails which can localize any single link failure. To overcome this problem, we adopt a well studied concept, *shared risk link group* (*SRLG*) [48], to represent a group of links that cannot be distinguished by the current proactive trail formation. Ideally, there is only one member in each shared risk link group. The process of our algorithm is simple. After the greedy trail formation, we proactively send labels along these chosen paths. If no link failure is detected, we move to the next round of proactive trail formation to cover those links with missing link labels. On the contrary, if a link failure is detected, a candidate failed link group would be uniquely identified. With the failed link group, the mesh topology fault localization problem has been transformed to linear topology which is much easier to solve.

Before illustration of the proactive failure detection algorithm, we first discuss the principle of formation of *SRLG*. In each wavelength plane λ , that is $G_\lambda(V_\lambda, E_\lambda)$, LM_λ is the set of LMs using wavelength λ . Those links whose link labels are not received in Phase 1, and are present distinctly in its own wavelength plane, are assigned to h_λ , where $h_\lambda \in H$ for all λ s. The algorithms, as illustrated in Fig. 3.3, are adopted to form a *monitoring trail* set, denoted as I_λ , that cover the links in h_λ . The breadth-first search algorithm is adopted, starting from each LM placed in $G_\lambda(V_\lambda, E_\lambda)$ until all the nodes connected to every LM are included in the same connected component. In graph theory, a connected component [49] of an undirected graph is a sub-graph in which any two vertices are connected to each other by paths, and which is connected to no additional vertices. Clearly, there are two possible

situations at this stage. One includes only single LM in the connected component, while the other contains multiple LMs. Thus, we have developed two heuristic forming policies, namely, *trail formation policy for connected graph with single LM* and *trail formation policy for connected graph with multiple LMs*, for trail formation under these two cases, respectively. Consequently, after all wavelength planes have been considered, an initial set of *SRLG*, denoted as I , where $I_\lambda \in I$ for all λ s, is formed as *proactive trails*.

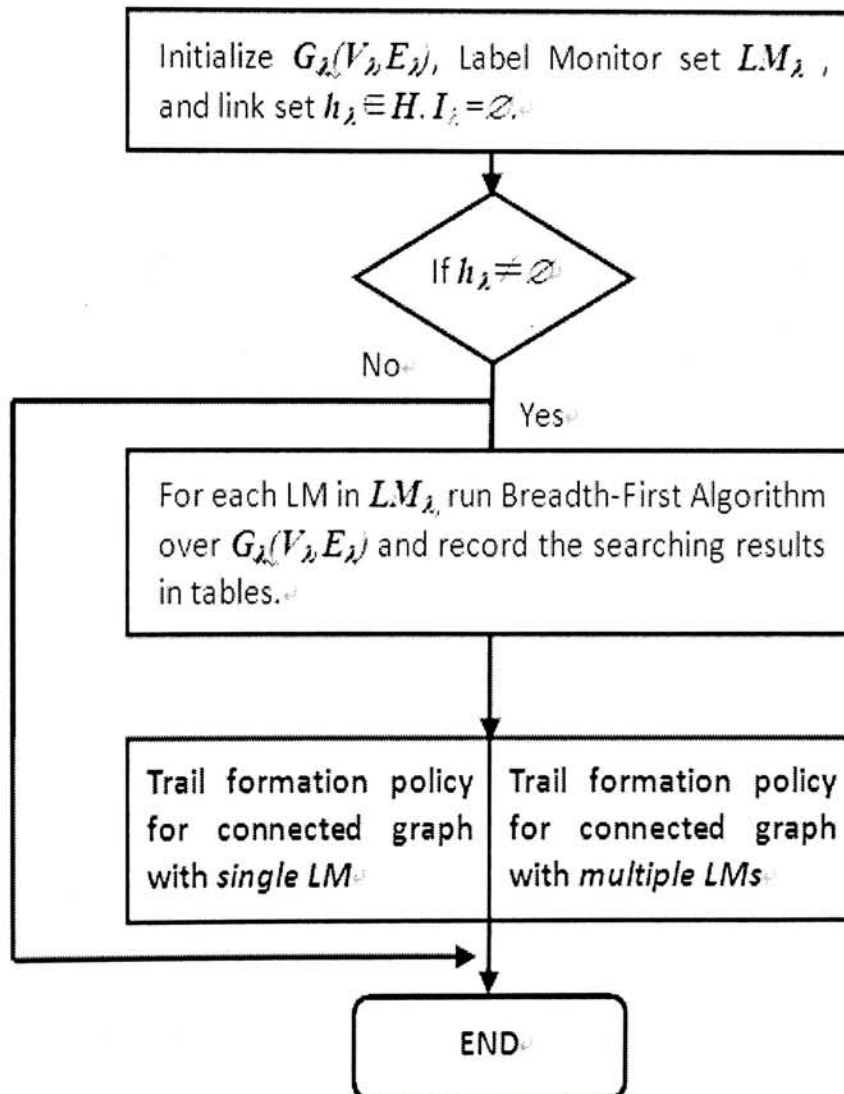


Fig. 3.3: Flowchart of the algorithm to form monitoring trail set in each wavelength plane

We present the details of the first heuristic, namely, *trail formation policy for connected graph with single LM* in the following table.

Trail formation policy for connected graph with single label monitor (LM)
<p>Step1: Reduce the original $G_\lambda(V_\lambda, E_\lambda)$ by eliminating those sub-graph component with no link $\in h_\lambda$.</p> <p>Step2: Using the obtained tables from the breadth-first searching algorithm in the previous step, starting from the only LM as the source,</p> <p> if (the first link $l \in h_\lambda$ is found)</p> <p> { form the trail t connecting l to the only label monitor with the shortest path.</p> <p> $h_\lambda = h_\lambda - l$;</p> <p> $I_\lambda = I_\lambda \cup t$;</p> <p> Go to Step3;</p> <p> }</p> <p> else go to Step4;</p> <p>Step3: Delete the trail t from $G_\lambda(V_\lambda, E_\lambda)$, update the tables from breadth-first searching algorithm, and go back to Step2.</p> <p>Step4: if ($h_\lambda = \emptyset$) go to Step5</p> <p> else { check whether if any links in h_λ can be connected to trails in I_λ.</p> <p> If yes, update I_λ.</p> <p> }</p> <p>Step5: Return I_λ</p> <p>END</p>

The Step 1 is used to eliminate those links and nodes that will never been used to form the trail in I_λ as there are no links belonging to h_λ around them. In step 2, we argue that we can use the result of previous breadth-first algorithm results to speed up trail form process. Generally, the heuristic is greedily forming trails covering links belonging to h_λ recursively by deleting used wavelength links from the original graph. The Step 4 is used to make sure that no links belonging to h_λ that could be easily add to the formed trail are missed, to maximize the number of links could be covered in I_λ .

We present the details of the second heuristic, namely, *trail formation policy for connected graph with multiple LMs* in the following table.

Trail Formation policy for connected graph with multiple label monitors (LMs)
<p>Step1: Reduce the original $G_\lambda(V_\lambda, E_\lambda)$ by eliminating those sub-graph component with no link $\in h_\lambda$</p> <p>Step2: Let $LM'_\lambda = LM_\lambda$</p> <p>Step3: Use the obtained tables from the breadth-first searching algorithm in the previous step. The search starts from every LM in LM'_λ over $G_\lambda(V_\lambda, E_\lambda)$. The nodes covered in every searching step have the same link distances to their respective source LMs.</p> <p>if (the first link $l \in h_\lambda$ is found in the searching path of a label monitor $m \in LM'_\lambda$)</p> <p>{ form the trail t connecting l to m with the shortest path;</p> <p>If multiple links exist, break the tie by choosing the link which will block the minimal number of uncovered links in h_λ to be formed in potential trails.</p> <p>$LM'_\lambda = LM'_\lambda - m$;</p> <p>$h_\lambda = h_\lambda - l$;</p> <p>$I_\lambda = I_\lambda \cup t$;</p> <p>Delete the trail t from $G_\lambda(V_\lambda, E_\lambda)$, update the tables from breadth-first searching algorithm, and go back to Step3</p> <p>}</p> <p>else {</p> <p>if ($h_\lambda = \emptyset$) go to Step4</p> <p>else { $LM'_\lambda = LM_\lambda - LM'_\lambda$;</p> <p>$LM_\lambda = LM'_\lambda$;</p> <p>if ($LM'_\lambda \neq \emptyset$) go back to Step3;</p> <p>else go to Step4</p> <p>}</p> <p>}</p> <p>Step4: For those remaining links in h_λ, check whether if any one of them can be connected to trails in I_λ</p> <p>if (yes), update I_λ</p> <p>Step5: Return I_λ</p> <p>END</p>

The general process is similar with the above algorithm except that we tend to distribute the trails to different LMs as it intuitively has better resource efficiency.

The initial set of SRLG, I , is then used as the input for the following *proactive failure detection algorithm*, as illustrated below.

Here are the notations in the *proactive failure detection algorithm*:

U : all the links that are not detected alive in Phase 1;

T : the selected proactive trails;

S : link set to be covered in T ;

Wp : the graph model showing free wavelength resource of the whole network;

L : As a subset of U , denoting those links that are not covered by T while through which at least one light-path can reach some LM in the current Wp .

Proactive Failure Detection Algorithm in Phase 2

Step0: $L=U$, and $S=\emptyset$

Let $T=I$

Update S , L and Wp

Step1: While $L \neq \emptyset$

 Select a link l randomly from L

 Compute a trail t passing through the nearest LM and l from Wp

$T=T \cup t$

 Update S , L and Wp

End

Step2: if a set of SLRG, p , appear in the same set of trails

 Sort the link group in p into different groups if there is at least one different trail t between any two different groups in Wp

$T=T \cup t$

End

Step3: Execute selected probing along the trails in T ;

 Return failure shared risk link group I^*

 if $I^*=\emptyset$

 if ($U \neq \emptyset$)

 {

 Update U and I according to T

 Return to Step0

 }

 else All links are alive

 else Failure_Location(I^*) //Failure_Location(.) is a function used to localize the exact location of fault within a shared risk link group//

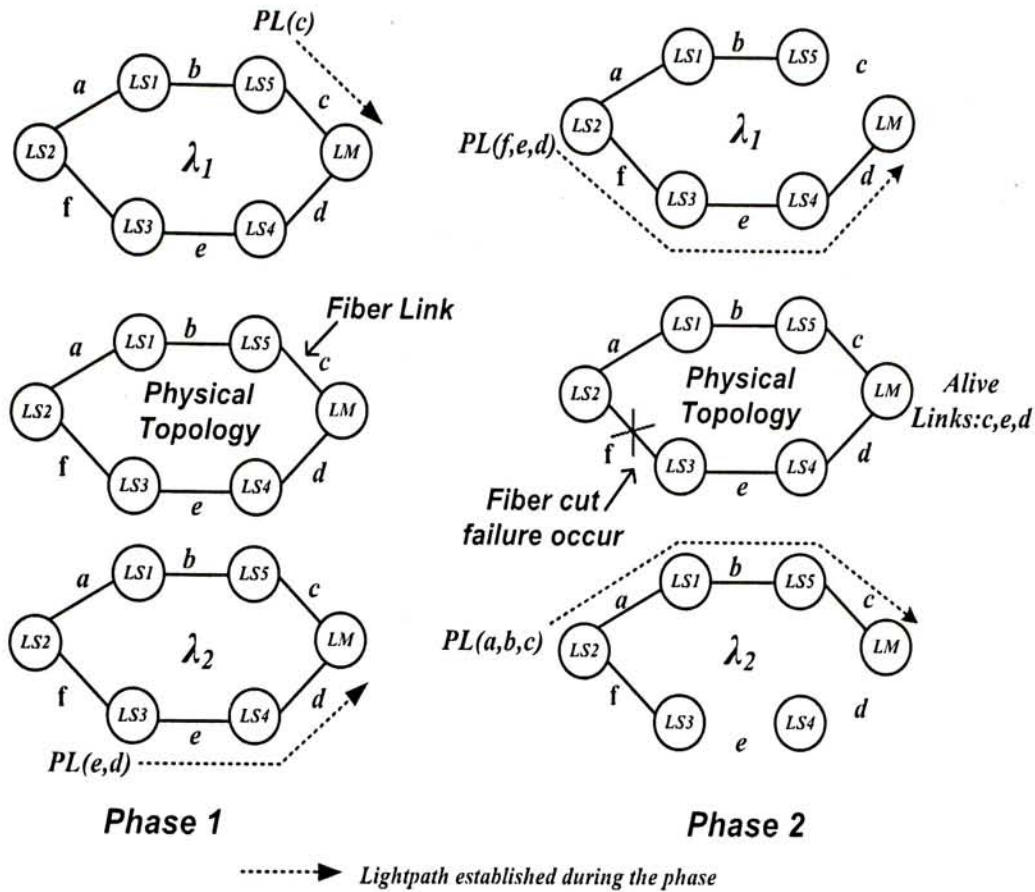


Fig. 3.4: An example to illustrate the procedures of Phase 2

To further illustrate this proactive failure detection algorithm, a simple example is shown in Fig. 3.4, where the six-node topology supports two wavelengths λ_1 and λ_2 . In this example, two light-paths are established in Phase 1, due to the real traffic requests. One is from LS5 to LM generating $PL(c)$ on wavelength λ_1 , while the other one is sourced at LS3 and sends $PL(e,d)$ to LM on wavelength λ_2 . As a result, the LM receives link label $LL\{c,e,d\}$ during Phase 1 and regards link c, e, d as currently active. At a certain time instant, the control plane checks the link label information at the LM to find that link labels, namely, a, b and f , have not yet received. Thus, we have $U=\{a,b,f\}$ and $L=U$. To completely diagnose all network link states, Phase 2, the proactive failure detection algorithm, is executed according to the result of Phase 1 and the current network wavelength resource. To accomplish that, first, we randomly

pick a link from those links with missing link labels, including a , b and f in L . We assume that f is selected, without loss of generality. Please note that the order in which links are selected does not affect our final failure localization results. Then a trail passing through the nearest LM and f is computed in the graph model. The trail is added to set T and those links with missing link labels along the trail is added to S . In the above case, one and the only one of the possible trail (f,e,d) on wavelength λ_1 is put into T , while link f is added to S . Now, updating the graph model means that the light-path from LS2 to LM on λ_1 plane is removed. Here, since link a and link b are still not covered and only one trail, passing through both of them, exists in the graph model, we will group the two links as a unique link group that can be treated as a virtual link, corresponding the updating set I in Step 3 of the algorithm. With this transformation, there is only one *SRLG* including physical links a and b in L , and therefore the same procedure is employed to this link class, as happened to link f . Thus, another trail (a,b,c) on wavelength λ_2 is added to T . This greedy proactive trail formation policy is performed until L is empty. In the above simple example, the two trails, (f,e,d) and (a,b,c) , can already locate the fiber failure at link f .

Obviously, for more complicated cases, those covered *SRLG* appeared in the same set of trails may arise after the initial trail formation procedure. To address this problem, if the unused wavelength resource is available, the algorithm will add new trails to distinguish these *SRLGs*. Otherwise, these *SRLGs* will be grouped as a larger *SRLG*. With this greedy proactive probing along the selected trails, we are able to uniquely identify a failed link group if a failure happens to those links covered in

proactive trail set T . If no failure happens, the algorithm will recursively update and probe the remaining un-covered links until a failure is identified or all the link labels are received.

3.2.4 Control Plane Design and Analysis

In this section, the design of the control plane will be discussed. Two important concepts, namely, Reliable Label (RL) and Reliable Time (RT), are defined to facilitate our discussions.

Reliable Label (RL): The labels stored at LMs which indicate the respective links are alive with probability p .

Reliable Time (RT): For each collected label at LMs, the time interval within which the label is treated as a RL from the instant the label is received.

Due to the intuitive fact that the occurrence probability of a link failure is getting larger when the respective link label is missing for a longer period of time, a threshold value for RT is selected to put probing effort on links with larger failure probability. The probability is determined by real network conditions and is monotonically decreasing with RT. Basically, RT is equivalent to the assumption used in [21] that the link state will not change during the proactive probing process, that is, within a certain time interval after the moment the label is detected. Thus, the previously detected link information will be reliable in the following proactive time. In the design of the control plane, network monitoring is performed in time intervals

of ΔT , as illustrated in Fig. 3.5. Within each time interval, a time instant is set as Check Point (CP), at which the system will check the RL list at LMs and make decisions for the execution of Phase 2. Phase 2 will be performed in the following time period between CP and the end of the current time interval ΔT , so as to limit the fault recovery time. At the end of Phase 2, fault notification will be issued if there is still any links with missing link labels. The time interval between two consecutive CP is also equal to ΔT . In case that Phase 1 and Phase 2 are performed in parallel, Phase 1 is collecting labels all the time, while Phase 2 periodically sends probes according to the RL list at each CP. Moreover, the longest time interval between failure occurrence and failure detection is bounded in our scheme, as explained in lemma 1.

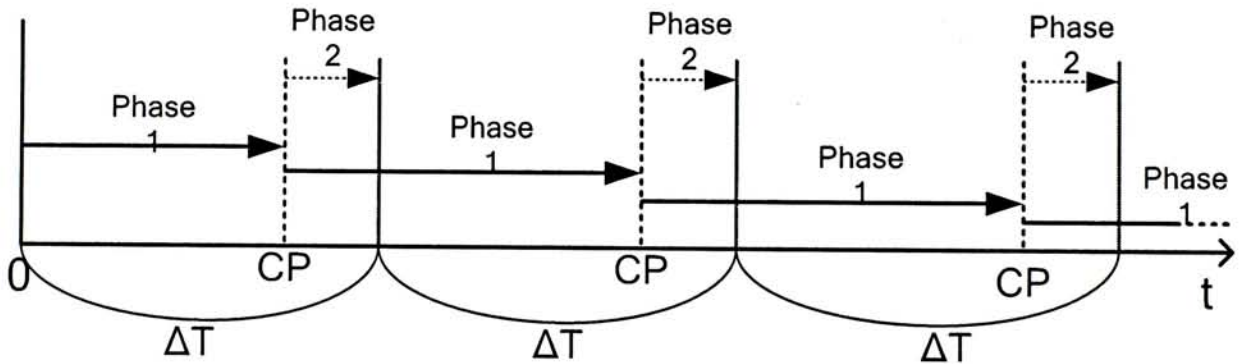


Fig. 3.5: Timeline of the proposed adaptive monitoring scheme

Lemma 1: *For any network topology, if all the nodes are LS, with at least one LM, single link failure localization time is bounded by $RT + \Delta T$*

Proof: In our fault localization scheme, the missing link label after Phase 2 corresponds to the failed link. From the start instant of each ΔT period, two possible situations for each link may occur. First, if there is at least one passive probe (light-path established in Phase 1) passing through it before being received at some

LMs, it will be detected at the first CP after its latest RT ends. Thus, if a link fails after its label having been collected at some LMs, the worst case would be that its RT ends just after a CP and this link is not included in any *shared risk link groups* in the following Phase 2 detection. In that case, an additional ΔT would be needed. Therefore, the worst case fault localization time would be $RT + \Delta T$. On the other hand, if there is no passive probe passing through certain links or a failure occurred before the passive probe is sent, the worst case fault localization time would be ΔT , since Phase 2 will be executed to detect the respective label for the failed link.

Lemma 1 proves that our fault detection and localization scheme is reliable and complete. By choosing RT and ΔT flexibly, our scheme can be adjusted adaptively according to different network link failure models and QoS specifications, in terms of reliability. For instance, the checktime interval ΔT can be reduced in a network that requires short recovery time. Hence, the system can locate the possible link failure within a shorter period. On the other hand, if the network operator is more concerned about the fault management cost than the recovery time, increasing ΔT can reduce the average amount of control messages sent in a certain period. Moreover, if fiber links in a particular network are exposed in a hostile or fast changing environment, the RT can be set to a smaller value. Besides, our scheme performs better when the real traffic load is getting higher, as more link labels will be received at the LMs in Phase 1. Hence, the network can improve the QoS, in terms of reliability, at about the same management cost.

3.2.5 Physical Layer Implementation and Suggestions

A path label will be sent out when a light-path has been established and the label will travel along the light-path along with the data. As the label is used to denote the path information of the light-path on a particular wavelength, there will be several light-paths going through the input port of the label monitor on different wavelengths. In order to gather the link label information from different light-paths, as much as possible, it will be desirable to have a low-cost label monitor, which can monitor the links labels on several different wavelengths, simultaneously. For example, subcarrier multiplexing may be employed to support multiple different labels, each of which are carried on a distinct subcarrier frequency. On the other hand, code-division multiple access (CDMA) is also a feasible alternative, as proposed in [50]. It integrates a direct-sequence CDMA (DS-SS) technique with a complementary constant weight code (CCWC). DS-SS is used to multiplex different link labels at baseband frequencies and CCWC is used to overlay the low-speed label into the high-speed payload. Instead of CCWC, Manchester coding or coded marked inversion (CMI) coding may also be used to encode the payload, such that there is a spectral null at DC, and thus enabling the insertion of the low-speed label.

3.3 Placement of Label Monitors

In the previous sections, we have illustrated the architecture and the principles of our adaptive fault monitoring system in an all-optical network. In this section, the LM

placement problem is discussed. It is shown that our scheme can be embedded into optical networks without any disturbance incurred to the data plane control. Moreover, among the three components (LS, LM and LL), the deployment cost of LM dominates the monitoring system cost. Therefore, it is highly desirable to minimize the number of the required label monitors and monitoring ports.

3.3.1 ILP Formulation

Problem Formation

Given a network topology $G(V,E)$, V represents the set of all nodes and E denotes the set of all links. Also, bidirectional fiber link is assumed. In our adaptive scheme, each link of the network uses a unique value as its link label (LL). As discussed in section 2, we simply assume that every node of the network is a label source (LS), since LS actually introduces negligible cost compared with the cost of LM. Our objective is to place the minimum number of monitors in the network, subject to the constraint that all link labels can be collected at LMs in Phase 1, if ΔT is long enough. To realize this objective, we present a simple placement solution formulated as an integer linear programming (ILP).

Minimum LM Placement

As discussed in sections 1 and 2, where and how the probes are sent in Phase 1 are determined by the data plane traffic and its routing method. Without loss of generality, the most common routing method, fixed-alternative k -shortest paths routing, for the data plane, is chosen, where k is set to be 2. Please note that, in this

ILP formulation, no actual traffic model parameters, such as the time interval distribution between two consecutive requests and holding time of requests are involved. We simply assume the traffic demands are uniformly distributed to all node pairs, indicating that all the k pre-computed paths will be used. In terms of future backbone all-optical networks, we believe the traffic nature would be increasingly dynamic. Yet, all other wavelength routing algorithms could be used and all possible traffic models could be adopted. The following formulation is an example, for illustration. The ILP is as follows:

$$\begin{aligned} \text{Minimize: } & \sum_{i \in V} N_i D_i \\ \text{Subject to: } & \sum_{i \in V} C_{ij} D_i \geq 1 \quad j \in E \end{aligned}$$

Notations:

V : The node set of the topology;

E : The link set of the topology;

N_i : Degree of node i ;

D_i : Placement binary variable. $D_i = 1$ means that node i is selected to place a LM; otherwise, $D_i = 0$;

C_{ij} : Binary input of the network. $C_{ij} = 1$ indicates that link j is included at least once by those two shortest paths between node i and all the other nodes.

In general, our objective is to minimize the overall number of LMs' ports subjected to the constraint that all the link labels could be possibly received at any LMs in Phase 1. Variable D_i represents the decision whether node i is selected to be LM. Since each LM should receive and monitor all the links attached to it, N_i , the degree of node i , is added as weight to include this property in the monitoring cost objective function which is to minimize. C_{ij} is a binary input value, indicating that if link j is included at least once by those two shortest paths between node i and all the other nodes. It can be achieved by offline computing the hop distance based 2 shortest

paths between every node pair, using Dijkstra algorithm. We would like to point out that the traffic from any of the other nodes to this LM is a broader concept because LM can collect labels that pass through it, in addition to those destined at this LM.

In the above ILP formulation input, k could be chosen to be other values. Larger k usually means smaller number of LMs required. Thus, the link status information collected in Phase 1 is reduced and this may increase the burden of Phase 2. Besides, the LM placement method could consider other alternative routing algorithms, such as adaptive dynamic routing, in which routing decision is made on the fly depending on the network wavelength resource. However, as there is no fixed route between the source and the destination in adaptive dynamic routing, a heuristic would be required to choose those hub nodes, for instance, via ranking the nodes with their node degrees.

3.3.2 Simulation Studies

In this section, we present the numerical results of our proposed framework and the comparison with M-Trail, which is a popular previously proposed solution for single link failure localization in all-optical networks.

ILP Formulation Results over Random Topology

We have applied our ILP formulation to a number of randomly generated topologies to evaluate the performance of our LM placement scheme. The network model was implemented using C/C++ with a free library, called *ip_solve*, included in Microsoft Visio Studio 2005. In the above ILP formulation input, the value of k was set to be 2.

The traffic demands were uniformly distributed to all node pairs. For different number of nodes, we start our placement from a ring topology (average node degree is 2) until a fully mesh network [25] is formed. For each average node degree value, denoted as AND , we randomly generated 100 topologies to get the average number of the monitor ports, which is set to be the cost value of our results, while the maximum monitor ports and the minimum monitor ports in those 100 topologies, are also presented. Fig. 3.6 and Fig. 3.7 show the monitor costs of different network sizes to realize Phase 1 function under AND values of 4 and 6. From Fig. 3.6 and Fig. 3.7, we have found that the monitor cost does not increase if the number of nodes and links maintaining the same average node degree. It is a very useful property, indicating that our adaptive scheme has great scalability, in terms of monitoring cost. The reason is also intuitive. As the number of links to be monitored increases, the number of LSs also increases by approximately the same ratio (AND). As the number of network nodes increases, the overall possible light-path in the network will also increase. Thus, those new links can be covered easily by the new possible light-path without extra monitoring cost. Fig. 3.8 puts the test results on networks with average node degree of 2, 4 and 6 in the same figure. Figs. 3.9, 3.10, 3.11, 3.12 and 3.13 show the monitor cost versus AND , for different number of nodes, together with the maximum and the minimum test results, in form of error bars, out of the 100 topologies used. Fig. 3.14 puts the test results on networks with node numbers of 6, 10, 14, 20 and 24, in the same figure. It is clear that our adaptive system cost increases with network AND , but not with the number of nodes. Moreover, the monitor cost is

shown to be relatively low in the *AND* interval between 2 and 5, which is within the *AND* interval in real networks.

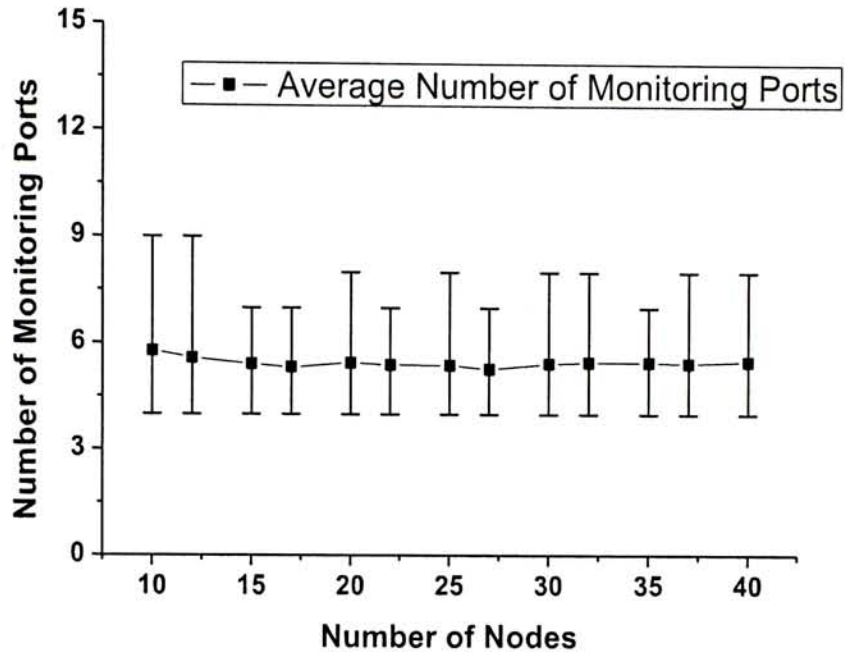


Fig. 3.6: Monitor cost(number of monitoring ports) versus node number with average node degree 4

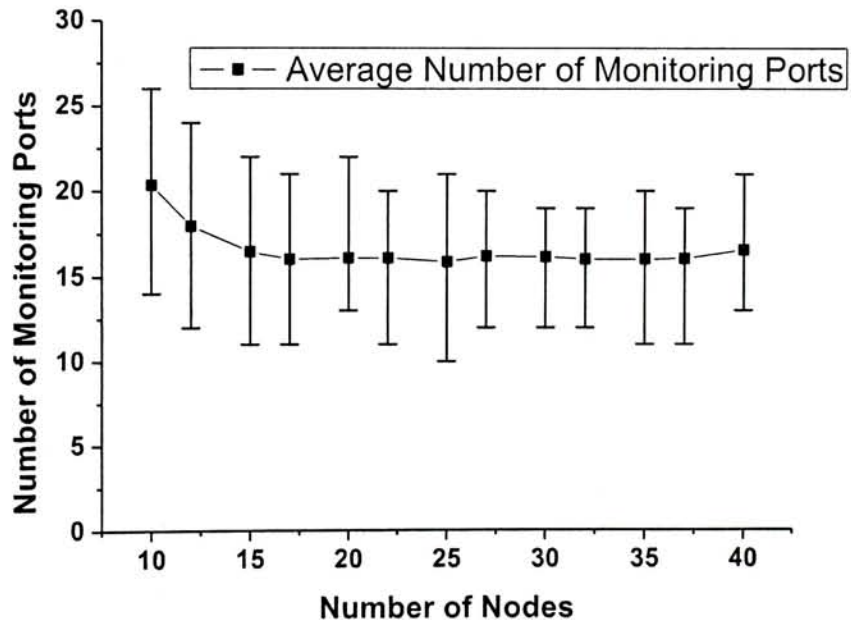


Fig. 3.7: Monitor cost(number of monitoring ports) versus node number with average node degree 6

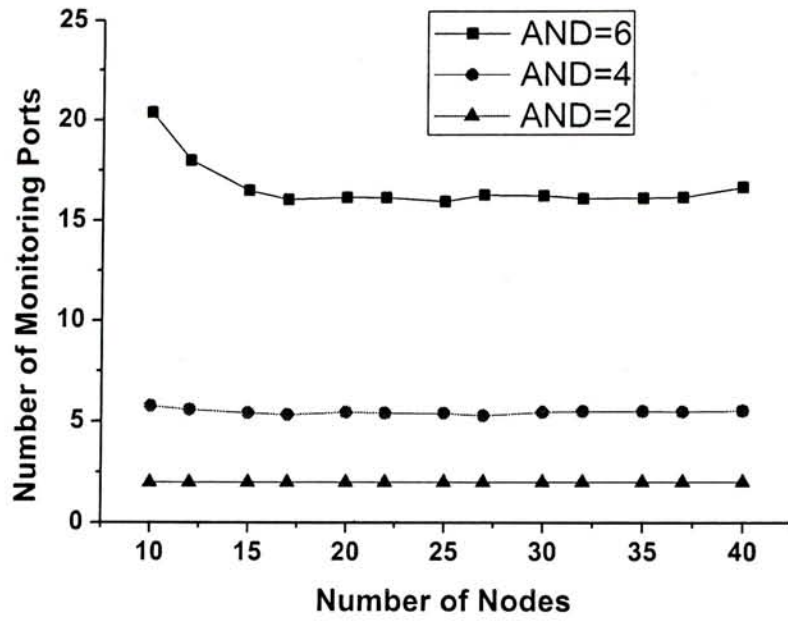


Fig. 3.8: Monitor cost(number of monitoring ports) versus node number with same average node degree (AND)

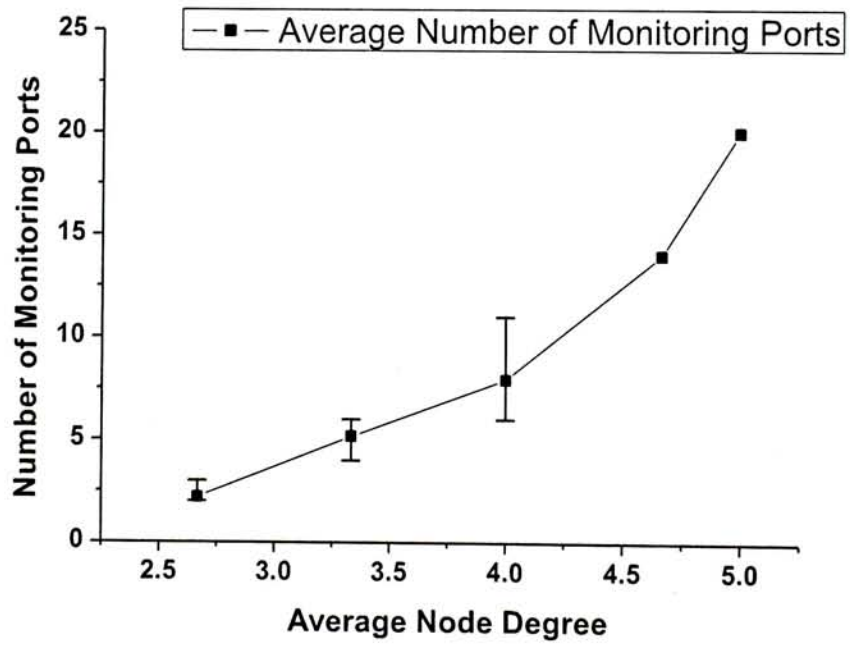


Fig. 3.9: Monitor cost(number of monitoring ports) versus AND with node number 6

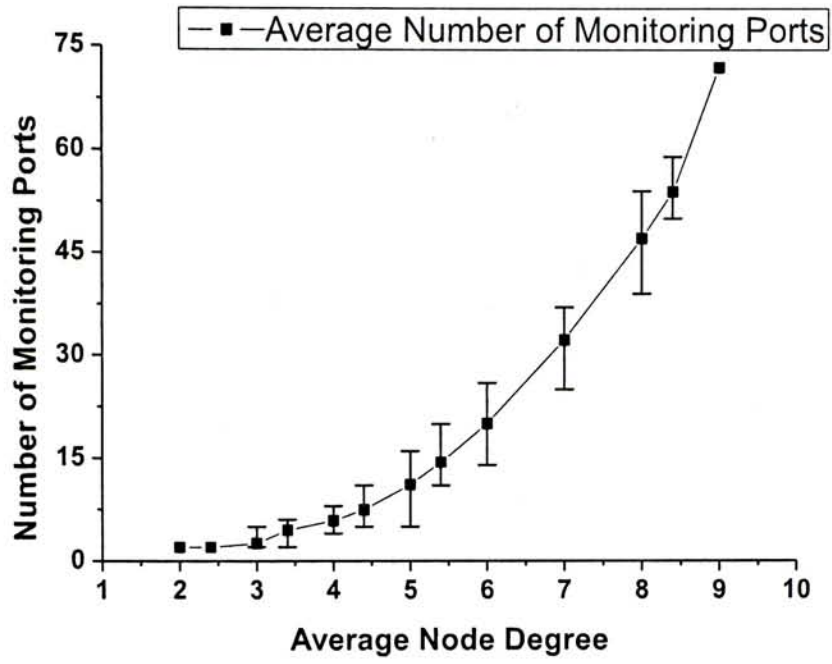


Fig. 3.10: Monitor cost(number of monitoring ports) versus AND with node number 10

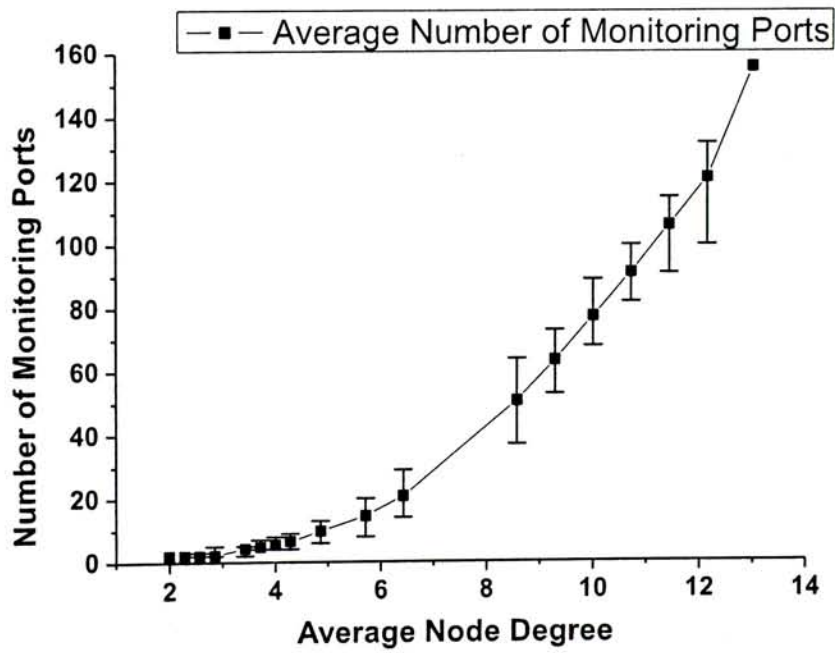


Fig. 3.11: Monitor cost(number of monitoring ports) versus AND with node number 14

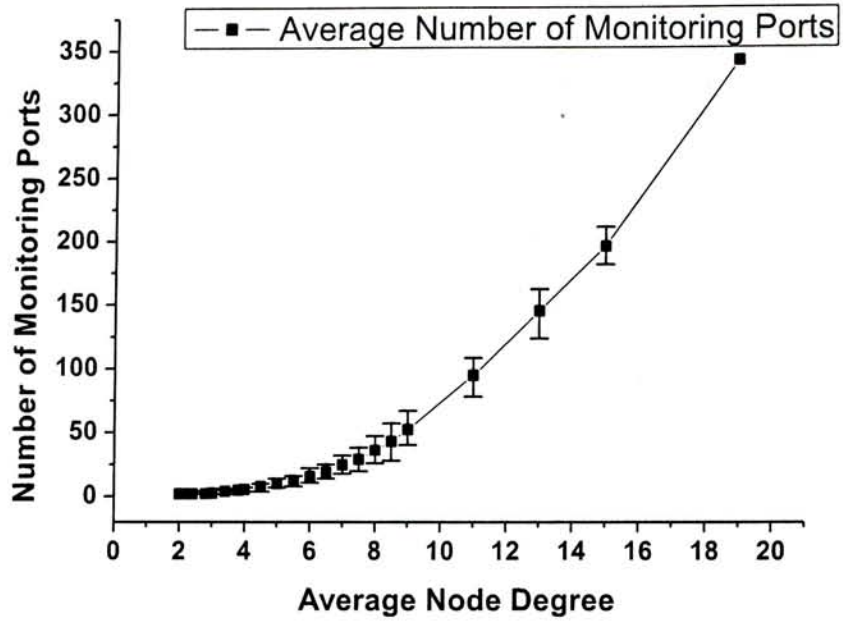


Fig. 3.12: Monitor cost(number of monitoring ports) versus AND with node number 20

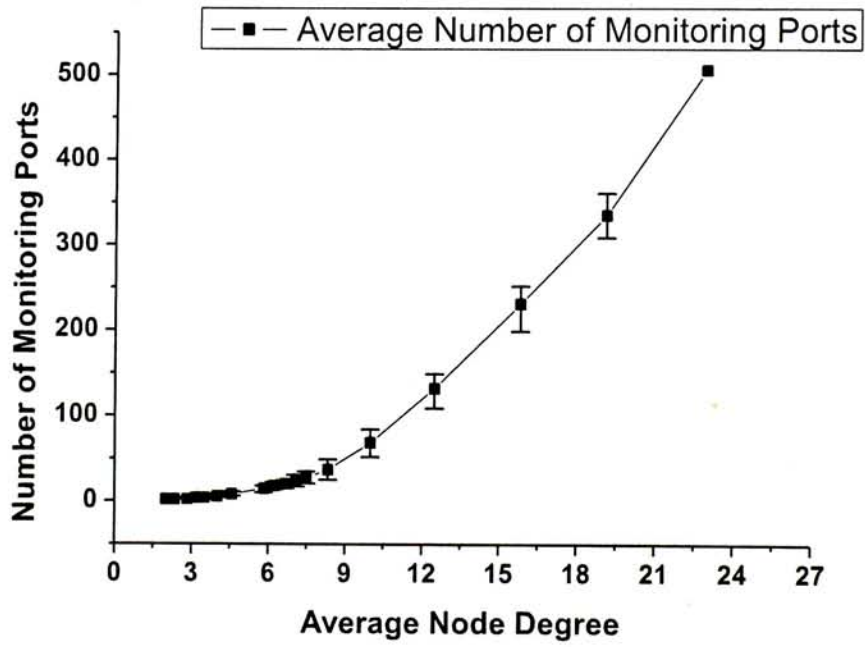


Fig. 3.13: Monitor cost(number of monitoring ports) versus AND with node number 24

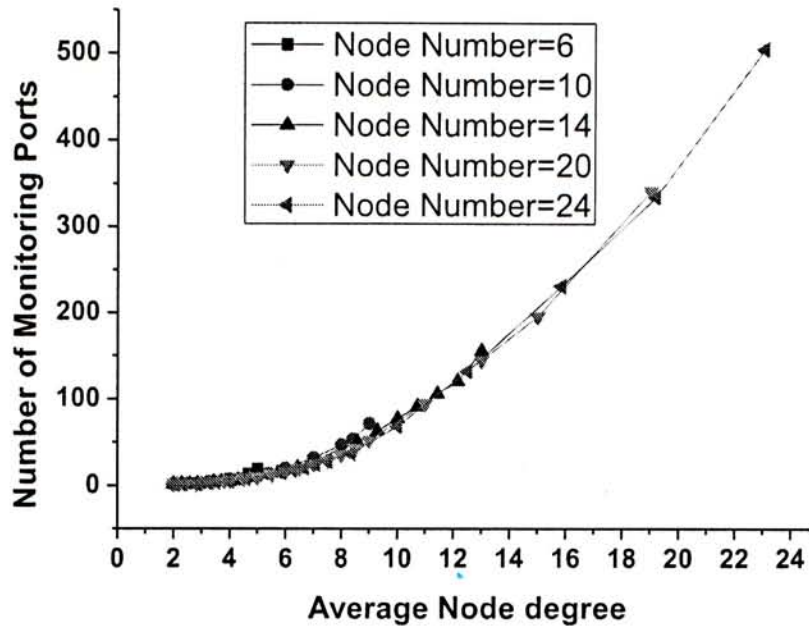


Fig. 3.14: Monitor cost(number of monitoring ports) versus AND with same node number

Monitoring Cost Comparison with M-Cycle and M-Trail Design

One major advantage of our adaptive monitoring framework, as compared with M-Trail and M-Cycle, is that almost no dedicated bandwidth is consumed for monitoring, since our adaptive scheme uses the free wavelengths of the data plane, while M-Trail and M-Cycle may require a significant number of dedicated monitoring channels, as the network dimension increases. Furthermore, the number of monitors required in our framework, M-Trail and M-Cycle are compared. Table 1 shows the results of our monitor placement, together with the respective data extracted from the original M-Cycle design and M-Trail design [24,27], for comparison. Several commonly used topologies, as shown in Fig. 3.15, are considered.

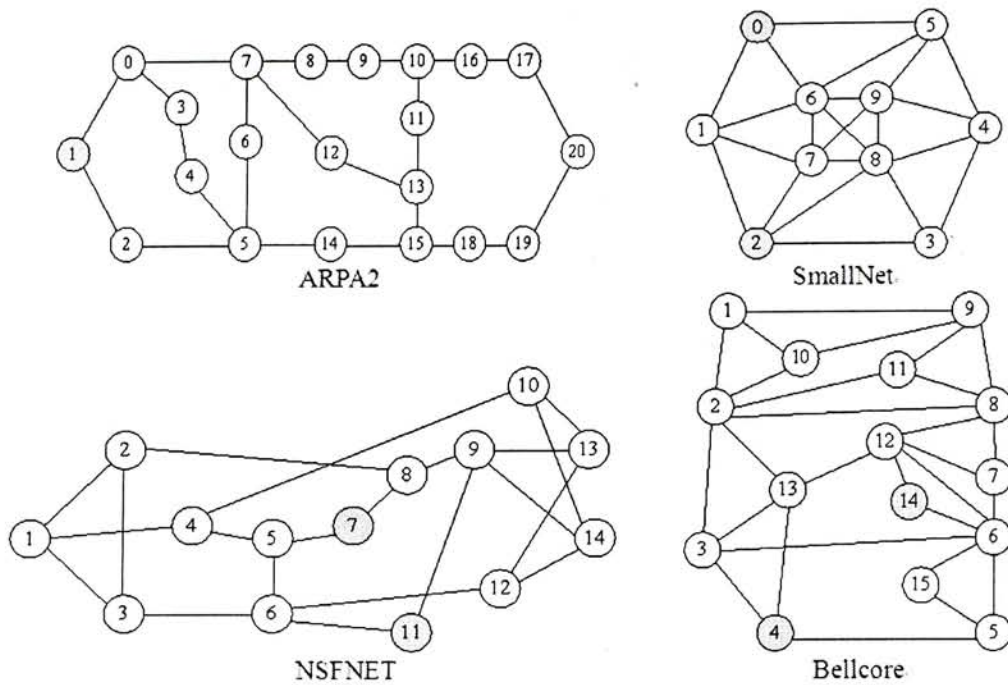


Fig. 3.15: Several commonly used topologies for monitor number comparison (shaded nodes denote monitoring locations using proposed scheme)

TABLE V MONITOR NUMBER COMPARISON WITH M-CYCLE[24] AND M-TRAIL[27]

Network topology	M-Cycle	M-Trail	Proposed Adaptive Scheme
ARPA2	20 cycles	11 trails	2 ports
SmallNet	13 cycles	6 trails	7 ports
NSFNET	10 cycles	Information not available*	4 ports
Bellcore	16 cycles	Information not available*	5 ports

*The authors are not able to find the references on the number of trails in those network topologies from available resources.

3.3.3 Discussion of Topology Evolution Adaptiveness

In the previous sections, we have presented a hybrid and adaptive fault localization framework which works by combining passive monitoring on real-time data traffic and proactive monitoring solutions together. By monitoring real-time data traffic in Phase 1, we can reduce the number of proactive probes in Phase 2. Moreover, the fast

changing real-time data traffic in optical networks will reduce the required number of

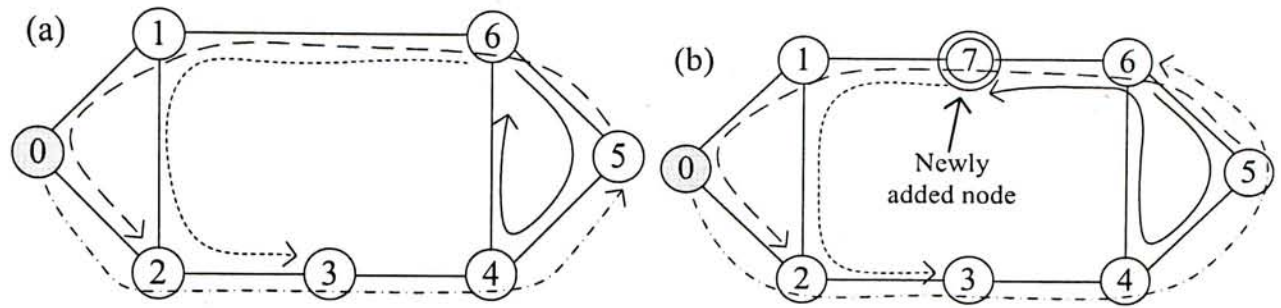


Fig. 3.16: Monitoring solutions updated using different monitoring schemes (proposed scheme and M-Trail) when network topology changes (a) the original network (b) the new network (shaded nodes denote monitoring locations using proposed scheme and arrows denote monitoring trails using M-Trail scheme)

fault monitors to be placed in the network, compared with previous passive monitoring schemes, which utilize static monitoring traces or routes, since a large amount of link states are monitored by a single label monitor in our scheme. In addition, it is noticed that the number of monitors to be placed in the network is proportional to the average node degree of the optical network. Hence, any insertion of network nodes will not increase the monitoring cost much as long as the average node degree of the optical network is maintained. Fig. 3.16 shows an example of how the monitoring solution changes when the network topology changes, i.e. addition or deletion of network nodes. In Fig. 3.16(a), M-trail scheme requires 4 trails marked by the different styles arrows, while our scheme requires the placement of the monitor at network node 0. When network node 7 is inserted to the network, as shown in Fig. 3.16(b), although the total number of trails can be kept constant, the trail configuration has to be changed. This leads to the change of the placement of monitors, lasers, and even the connection pattern of the supervisory channel at the network nodes. Nevertheless, our scheme requires no additional modification, in this example. Further analysis will be

conducted to examine the robustness of our proposed scheme under network topology changes. Besides, M-trail's ILP calculation [27] requires large number of constraints, which increases the complexity of computation. The situation would get even worst for network with larger dimension. Due to the ease of the computation of the monitor location of our scheme, much less computation time is required whenever there are changes in the network topology.

3.4 Summary

We have proposed a novel and practical adaptive fault monitoring scheme in all-optical networks based on label tracing monitoring (LTM) method. A simple yet effective monitor placement method using ILP is presented. Our results show that our adaptive fault localization scheme has great scalability in terms of the lowest number of fault monitors required. Besides, our scheme performs better, in terms of design flexibility and minimal additional dedicated monitoring bandwidth, than the common passive monitoring solutions.

Chapter 4 Conclusions and Future Work

4.1 Conclusions

Two important aspects of optical networks have been investigated, in this thesis.

To alleviate the physical layer impairments influence induced by current stage optical transmission technology, as well as achieve cost-effective light-path provision, we have first explored a novel sparsely placed regeneration site based translucent optical network architecture employing heterogeneous modulation format under two problem settings, and have used several numeric studies to verify our cost-saving expectations; Then, we have proceeded to study the regenerator placement problem in selective regeneration architecture, together with a traffic grooming objective. By constructing a graph incorporating regenerator placement and traffic grooming, and manipulating the weights of those links in the graph, we can simply run shortest path algorithm over that graph to know where to route over the network, where to use existing available multiplexing wavelength connection channels, whether/where to create new multiplexing wavelength connections, where to add regenerators, and what is the overall investment cost: all the information a planner would like to know, defined as routing policy. Simulation results clearly have demonstrated the correctness of our approach; on the other hand, we have described and identified a new optimization opportunity in reducing the number of regenerators needed for wavelength conversion. Based on the same design philosophy, an auxiliary graph is built to fully explore the optimization opportunity,

and consequently, substantial cost saving is achieved through extensive network data simulation.

The chapter 2 is dedicated to tackle the “Quality of Transmission” problem for current technology stage, to some extent, while chapter 3 is the first effort to expand conventional fault monitoring framework horizon, a crucial part to ensure “Quality of Service”, by combining two popular existing schemes, that is passive monitoring and proactive monitoring, in future all-optical networks.

4.2 Future Work

First, although ILP can find the optimal solutions to the regeneration site and transponder placement problem in 2.2.3, it generally requires intractable computing time, meaning that we have to develop efficient heuristic to handle large scale of problem sets, which happened to be our next investigation stop.

In addition, other than the original objective, we also plan to study the impact of using different modulation formats for adjacent channels. Hopefully, we can propose an integrated solution to solve the planning problem while minimizing the influence induced by heterogeneous modulation format, if any.

As for the adaptive fault monitoring framework, we plan to further quantify the time line analysis with control plane message processing protocol if practical failure cases and services are present.

Bibliography

- [1] G. Shen and R. S. Tucker, "Translucent optical networks: The way forward," *IEEE Commun. Mag.*, vol. 45, no. 2, pp. 48–54, Feb. 2007.
- [2] A. Saleh, "Island of Transparency — An Emerging Reality in Multi-wavelength Optical Networking," *Proc. IEEE/LEOS Summer Topical Meeting on Broadband Opt. Net. and Tech.*, July 1998, p. 36.
- [3] E. Karasan and M. Arisoylu, "Design of translucent optical networks: Partitioning and restoration," *Photon. Netw. Commun.*, vol. 8, no. 2, pp. 209–221, Feb. 2004.
- [4] G. Shen, Wayne V. Sorin, and Rodney S. Tucker, "Cross-Layer Design of ASE-Noise-Limited Island-Based Translucent Optical Networks," *IEEE/OSA J. Lightwave Technology*, vol. 27, no. 11, June 2009, pp. 1434-1442.
- [5] X. Yang and B. Ramamurthy, "Sparse regeneration in translucent wavelength routed optical networks: architecture, network design and wavelength routing," *Photon. Netw. Commun.*, vol. 10, pp. 39-53, 2005.
- [6] T. J. Carpenter, R. C. Menendez, D. F. Shallcross, J. Gannett, J. Jackel, and A. V. Leh Lehmen, "Maximizing the transparency advantage in optical networks," in *Proc. OFC'03*, 2003.
- [7] A. Sen, S. Murthy, and S. Bandyopadhyay, "On sparse placement of regenerator nodes in translucent optical networks," presented at the *Proc. Globecom'08*, New Orleans, LA.

- [8] G. Shen, et al., "Cross-Layer Traffic Grooming for Optical Networks with Hybrid Layer-One and Layer-Zero Signal Regeneration", in *Proc. OFC'10*, Mar.2010.
- [9] W. Zhang, J. Tang , K. Nygard, C. Wang, "REPARE: Regenerator Placement and Routing Establishment in Translucent Networks," in *Proc. GLOBECOM'09*, 2009.
- [10]M. Youssef, S. Zahr, and M. Gagnaire, "Traffic-Driven vs. Topology-Driven Strategies for Regeneration Sites Placement," in *Proc. ICC'10*, 2010.
- [11]G. Shen et al., "Sparse placement of electronic switching nodes for low blocking in translucent optical networks," *OSA J. Opt. Netw.*, vol. 1, no. 12, pp. 424–441, Dec. 2002.
- [12]X. Yang, L. Shen, and B. Ramamurthy, "Survivable lightpath provisioning in WDM mesh networks under shared path protection and signal quality constraints," *IEEE/OSA J. Lightwave Technology*, Vol. 23, no. 4, pp. 1556, Apr. 2005.
- [13]G. Shen and W. D. Grover, "Segment-based approaches to survivable translucent network design under various ultra long haul system reach," *OSA J. Opt. Netw.*, vol. 3, no. 1, pp. 1–24, Jan. 2004.
- [14]K. Zhu and B. Mukherjee, "Traffic grooming in an optical WDM mesh network," *IEEE JASC*, vol. 20, no. 1, pp. 122-133, Jan. 2002.
- [15]H. Zhu, et al., "A novel graph model for dynamic traffic grooming in WDM mesh networks", *Proc Globecom '02*, Taipei, Nov. 2002.

- [16]K. Zhu, H. Zhang, and B. Mukherjee, "Design of WDM mesh network with sparse grooming capability," in *Proc. Globecom '02*, 2002, pp. 2696–2700.
- [17]G. Shen and Rodney S. Tucker, "Sparse Traffic Grooming in Translucent Optical Networks," *IEEE/OSA J. Lightwave Technology*, vol. 27, no. 20, Oct. 2009, pp. 4471-4479.
- [18]A. S. Arora and S. Subramaniam, "Converter placement in wavelength routing mesh topologies," in *Proc. IEEE ICC*, June 2000, pp.1282–1288.
- [19]Angela L.Chiu,et al, "Restoration design in IP over reconfigurable all-optical networks," *NPC 2007*,315-333.
- [20]C. Assi, Y. Ye, A. Shami, S. Dixit and M. Ali, "A hybrid distributed fault-management protocol for combating single-fiber failures in mesh-based DWDM optical networks," in *Proc. IEEE Globecom' 02*, Nov.2002, vol. 3, pp. 2676-2680.
- [21]Y.G. Wen, V. W. S. Chan and L. Z. Zheng, "Efficient fault diagnosis algorithms for all-optical WDM networks with probabilistic link failures," *IEEE/OSA J. Lightwave Technology*, Vol. 23, No. 10, Oct. 2005, pp.3358-3371, (invited paper).
- [22]M. Goyal, K. K. Ramakrishnan, and W.-C. Feng, "Achieving faster failure detection in OSPF networks", in *Proc. IEEE ICC' 03*, May 2003, vol. 1, pp. 296-300.
- [23]S. Stanic, S. Subramaniam, H. Choi, G. Sahin and H.-A. Choi, "On monitoring transparent optical networks," in *Proc. Int'l Conf. on Parallel Processing*

- Workshops*, Aug. 2003, pp. 217-223.
- [24]H. Zeng, C. Huang, and A. Vukovic, "A novel fault detection and localization scheme for mesh all-optical networks based on monitoring-cycles," *Photon. Netw. Commun.*, vol. 11, no. 3, pp. 277–286, May 2006.
- [25]J. Tapolcai, B. Wu, and P.-H. Ho, "On monitoring and failure localization in mesh all-optical networks," in *Proc. IEEE INFOCOM 2009*, Apr. 2009, pp. 1008–1016.
- [26]B. Wu, K. L. Yeung and P.-H. Ho, "Monitoring cycle design for fast link failure localization in all-optical networks," *IEEE/OSA J. Lightwave Technology*, vol. 27, no. 10, pp. 1392-1401, May 2009.
- [27]B. Wu, P.-H. Ho and K. L. Yeung, "Monitoring trail: on fast link failure localization in all-optical WDM mesh networks," *IEEE/OSA J. Lightwave Technology*, vol. 27, no. 18, pp. 4175-4185, Sept. 2009.
- [28]Y.Wen et al., "Non-Adaptive Fault Diagnosis for All-Optical Networks via Combinatorial Group Testing on Graphs," in *Proc. IEEE INFOCOM 2007*.
- [29]R. Ramaswami and K. Sivarajan, *Optical Networks: A Practical Perspective*, 2nd ed. San Mateo, CA: Morgan Kaufmann, 2002.
- [30]Jane M Simmons, *Optical Network Design and Planning*, Boston, MA: Springer-Verlag US, 2008.
- [31]T. Carpenter, D. Shallcross, J. Gannett, J. Jackel, and A. Lehmen, "Method and system for design and routing in transparent optical networks," U.S. Patent 7,286,480 B2, Oct., 2007.

- [32]A. Nag, M. Tornatore, and B. Mukherjee, "Optical network design with mixed line rates and multiple modulation formats," presented at the *OFC'09*, San Diego, CA, Mar. 2009, Post-deadline Papers.
- [33]K. Christodoulopoulos, K. Manousakis and E. Varvarigos, "Adapting the Transmission Reach in Mixed Line Rates WDM Transport Networks," presented at *Optical Network Design and Modeling (ONDM)*, 2011 15th International Conference on .
- [34]M.A. Ezzahdi, S. Al Zahr, M. Koub`aa, N. Puech, M. Gagnaire, "LERP:a quality of transmission dependent heuristic for routing and wavelength assignment in hybrid WDM networks," in *Proc. IEEE ICCCN'06*, 2006, pp. 125–130.
- [35]B. Mikkelsen, C. Rasmussen, P. Mamyshev, F. Liu, S. Dey, F. Rosca, "Deployment of 40 Gb/s systems: technical and cost issues," *OFC'04*, paper THE6.
- [36]A. A. M. Saleh, J. M. Simmons, "Evolution toward the next-generation core optical network," *IEEE/OSA J. Lightwave Technology*, vol. 24, no. 9, pp. 3303-3321, Sep. 2006.
- [37]A. Morea, N. Brogard, F. Leplingard, J. C. Antona, T. Zami, B. Lavigne, and D. Bayart, "QoT function and A* routing an optimized combination for connection search in translucent networks," *J. Opt. Netw.*, vol. 7, no. 1, pp. 42–61, 2008.
- [38]G. Shen and R. S. Tucker, "Energy-minimized design for IP over WDM networks," *J. Opt. Netw*, vol. 1, no. 1, pp. 176–186, 2009.

- [39]X. Liu, S. Chandrasekhar, “High Spectral-Efficiency Mixed 10G/40G/100G Transmission”, *OFC'08, 2008*.
- [40]T. J. Xia et. al., “Multi-Rate (111-Gb/s, 2x43-Gb/s, and 8x10.7-Gb/s) Transmission at 50 GHz Channel Spacing over 1040-km Field-Deployed Fiber”, *ECOC'08, 2008*.
- [41]C. Meusburger, D. A. Schupke, “Optimizing the Migration of Channels with higher Bit-rates”, *OFC'09, 2009*.
- [42]Guangzhi Li, Chiu,A. , Doverspike,R., Dahai Xu , Dongmei Wang, “Efficient routing in heterogeneous core DWDM networks”,*OFC'10,2010*, paper NTHE3.
- [43]Angela L. Chiu.,et al., “Network Design and Architectures for Highly Dynamic Next-Generation IP-Over-Optical Long Distance Networks”, *OFC'09,2009*, San Diego, CA, March 2009.
- [44]V. W. S. Chan, et al, “A precompetitive consortium on wide-band all-optical networks,” *IEEE/OSA J. Lightwave Technology*, Vol.11, No. 5/6, May/Jun., 1993, pp. 714-735.
- [45]M. W. Maeda, “Management and control of transparent optical networks,” *IEEE J. Sel. Areas Commun.*, vol. 16, no. 7, pp. 1008–1023, Sep. 1998.
- [46]A. Jajszczyk, P. Rozycki, “Recovery of the control plane after failures in ASON/GMPLS Networks”, *IEEE Network*, Vol.20, No.1, Jan/Feb 2006
- [47]S. Ahuja, S. Ramasubramanian and M. Krunz, “Single link failure detection in all-optical networks using monitoring cycles and paths,”*IEEE/ACM Trans. on Networking*, Vol. 17, No. 4, Aug. 2009, pp.1080-1093.

[48]J. Strand, A. Chiu, and R. Tkach, "Issues for routing in the optical layer," *IEEE Commun. Mag.*, vol. 39, pp. 81–87, Feb. 2001.

[49][http://en.wikipedia.org/wiki/Connected_component_\(graph_theory\)](http://en.wikipedia.org/wiki/Connected_component_(graph_theory)).

[50]V. A. Vaishampayan, M. D. Feuer, "An overlay architecture for managing lightpaths in optically routed networks," *IEEE Trans. Commun.*, vol. 53, no. 10, pp. 1729-1737, Oct. 2005.

Publications during M.Phil Study

Published:

- [1] **D. Shen**, G.Z. Li, A. Chiu, D.M. Hwang, D.H. Xu, D.M. Wang, C.K. Chan and R. Doverspike, "On Multiplexing Optimization in DWDM Networks," in *OFC/NFOEC 2011*, Paper OTuR3, Los Angeles, USA, Mar. 2011.
- [2] **D. Shen**, G.Z. Li, A. Chiu, D.M. Wang, C.K. Chan and R. Doverspike, "Efficient Regenerator Placement and Wavelength Assignment in Optical Networks," in *OFC/NFOEC 2011*, Paper OThAA4, Los Angeles, USA, Mar. 2011.
- [3] **D. Shen**, S.Q. Zhang, C.K. Chan, "Design of Translucent Optical Network using Heterogeneous Modulation Formats," in *Proc. OptoElectronics and Communications Conference, OECC 2010*, Paper 8P-09, Sapporo, Hokkaido, Japan, 2010.
- [4] S. Q. Zhang, **D. Shen**, C. K. Chan, "Energy Efficient Time-Aware Traffic Grooming in Wavelength Routing Networks," in *GLOBECOM 2010*, Miami, Florida, USA, Dec. 2010.
- [5] W. Jia, **D. Shen**, K.H. Tse, J. Xu, M. Li and C. K. Chan, "A Novel Scheme to realize a Power-efficient WDM Passive Optical Network," in *Proc. OptoElectronics and Communications Conference, OECC 2010*, Paper 8A-34, Sapporo, Hokkaido, Japan, 2010.
- [6] S. Q. Zhang, **D. Shen**, C. K. Chan, "Energy Efficient Traffic Grooming in WDM Networks with Scheduled Time Traffic," *IEEE/OSA J. Lightwave Technology*, 2011.

In submission:

[1] **D. Shen**, K.H. Tse, C. K. Chan, “Adaptive Fault Monitoring in All-Optical Networks Utilizing Real-Time Data Traffic,” submitted to *Journal of Network and system Management*, under review after first revision.

[2] **D. Shen**, C. K. Chan, “Translucent Optical Network Planning Employing Multiple Modulation Formats,” to be submitted to *IEEE/OSA Journal of Lightwave Technology*.

CUHK Libraries



004777726